



**CYCLONE
TESTING
STATION**



FOR A SAFER STATE

Tropical Cyclone Ilsa – Wind field and damage to buildings in the East Pilbara

CTS Technical Report No 67



Cyclone Testing Station
College of Science and Engineering
James Cook University
Queensland, 4811, Australia
www.jcu.edu.au/cyclone-testing-station

CYCLONE TESTING STATION

**College of Science and Engineering
JAMES COOK UNIVERSITY**

TECHNICAL REPORT NO. 67

Tropical Cyclone Ilsa

Wind field and damage to buildings in the East Pilbara

Dr Geoff Boughton¹, Debbie Falck¹, Dr John Ginger¹, Dr David Henderson¹, Lucas van Woensel²

Cyclone Testing Station, James Cook University, Townsville

¹ Cyclone Testing Station.

² WA Department of Mines, Industry Regulation and Safety

9 June 2023

© Cyclone Testing Station, James Cook University

Bibliography.

ISBN 978-0-6457422-5-1

ISSN 1058-8338

Series: Technical Report (James Cook University, Cyclone Testing Station); XX

Notes: Bibliography

Investigation Tropical Cyclone Ilsa – Wind field and damage to buildings in the East Pilbara

1. Cyclone Ilsa 2023 2. Wind field 3. Damage to solar panels 4. Damage to sheds 5. Damage to buildings – Natural disaster effects 6. Wind damage

LIMITATIONS OF THE REPORT

The Cyclone Testing Station (CTS) has taken all reasonable steps and due care to ensure that the information contained herein is correct at the time of publication. CTS expressly excludes all liability for loss, damage or other consequences that may result from the application of this report.

This report may only be published in full if the publication of an abstract includes a statement directing the reader to the full report.

Executive Summary

Severe Tropical Cyclone Ilsa (TC Ilsa) crossed the coast on the northern border of wind region D and caused damage to several small remote communities including a roadhouse, cattle stations and mine sites. The Cyclone Testing Station, the WA Department of Mines Industry Regulation and Safety's Building and Energy Division (Building and Energy) and the WA Department of Fire and Emergency Services conducted an investigation to establish the wind field in the area affected and examine damage to buildings.

Anemometers, road signs (used as peak gust "windicators"), vegetation damage, the information provided by residents and a numerical model of cyclone wind speeds all contributed to the development of the maximum wind speed map. It showed that the peak 0.2-sec wind gust in standard conditions was higher than V_{500} from AS/NZS 1170.2:2021 as it crossed into each of wind regions. Because TC Ilsa crossed at the northern boundary of wind region D, the estimated maximum wind speeds in the coastal strip of wind region C exceeded 120% of V_{500} . The estimated maximum wind speeds in TC Ilsa as it moved into wind region A were also higher than 120% of V_{500} . The observed storm tide was around the Highest Astronomical Tide level and caused no damage to buildings.

Many solar panel systems throughout the study area sustained significant damage caused by bending failure of the panels, failure of the connection between the panels and the supporting frame, and failure of the connection between the roof-mounted panel support rails and the roof. Damaged solar panels became wind-borne debris that damaged other solar panels or buildings. The design criteria and testing of solar panel mounting systems needs to be reviewed for all wind regions because solar panels are a major part of Australia's transition to renewable energy.

The structural performance of many sheds under wind actions was poor. It appeared that some were not designed for the appropriate wind region, terrain and topography. Design of open sheds should include provision for blockage by contents or use appropriate internal pressures.

Dongas (transportable accommodation) need to have appropriate wind ratings, be well anchored to footings with appropriate mass and add-on structures such as verandas must be well-engineered. When purchasing and relocating a used donga, it is particularly important to confirm that the wind rating on the building is sufficient for its new site and to engineer the tie-down system and footings for the new wind environment.

Resilient buildings with good protection for windows and openings performed well during TC Ilsa. Buildings built for a higher wind region also performed well. This event showed that this is an effective way of building-in resilience, especially for locations close to a wind region boundary. However, where failures in buildings occurred, the cause was frequently because of deterioration of structural elements or the use of lightweight steel framing of inadequate thickness. Connections in steel-framed construction rely on sufficient steel thickness in framing members to provide adequate capacity and maintenance of all buildings is important.

Acknowledgements

The authors thank the residents of the Pilbara communities and mining companies who generously assisted with this study by volunteering information and inviting the authors onto their properties.

During this investigation, the CTS team worked closely with Building and Energy, and the Department of Fire and Emergency Services (DFES) WA. The collaboration between the three organisations enabled a coordinated, efficient, and effective approach to the investigation that increased the amount of data and information gathered. The outcomes of the study will ultimately contribute to improved community resilience to future tropical cyclones in all parts of Australia.

The authors particularly acknowledge the support given by:

- **Building and Energy** – particularly Kishor Dabasia, Allan Shiell, Mark Riordan, Sean de Prazer, Nabil Yazdani and Lindy Chew.
- **DFES** – provided information and data on the location of damaged properties and contact details of people in the area that could facilitate visits to properties. The team particularly appreciated the assistance of Su Groome, Justin Whitney, Adrian Brannigan, Peter Cameron and also Steve Gray of National Emergency Management Agency (NEMA).
- **Shire of East Pilbara** – Wendy McWhirter-Brooks (Deputy Shire President), Steven Harding (CEO), David and Catherine Olney (Shire rangers at Cape Keraudren).
- **Ashburton Aboriginal Communities** – Wendy Lyman (Manager).
- **Dr Bruce Harper of SEA** and Adjunct Professor at James Cook University for assistance with data and modelling to estimate the wind field.
- **The Bureau of Meteorology** – especially Joe Courtney for assistance in interpreting meteorological data and providing the track of TC Ilsa, and Andrew Burton and Adam Conroy for providing feedback and the BoM summary information.
- **Station owners and Managers in the affected area** –particularly Glen Goding (Pardoo Station), Belinda and Lux Lethbridge (Warrawagine Station), Annabelle Coppin (Yarrie Station), and Lance and Anna Coppin (Muccan Station).
- **Pilbara Development Commission** – Terry Hill (CEO).
- **Newcrest Mining Limited** (Telfer) – particularly Stephen Fitch, Lauren Van Den Crommenacker, Ian Lang, and Ivan Wong.
- **BHP Yarrie Mine** – Craig Drummond and Scott Burling.
- **Horizon Power** – Stephen Kiernan (Marble Bar Solar), Tori Fitzgerald (Port Hedland).

The CTS is grateful for the financial support by DFES, Building and Energy WA, Queensland Department of Energy and Public Works, and the CTS Sponsors and Benefactors.



FOR A SAFER STATE



Queensland Government



Table of contents

1. INTRODUCTION	9
1.1. Severe Tropical Cyclone Ilsa Overview	9
1.2. Purpose of the report	9
1.3. Investigation	9
2. SEVERE TROPICAL CYCLONE ILSA	10
2.1. Generation and predictions	10
2.2. Track	11
2.3. Anemometer data	11
3. ESTIMATING THE TC ILSA WIND FIELD	13
3.1. Field investigation	13
3.1.1. TC Ilsa track	13
3.1.2. Evaluation of road signs	15
3.2. Numerical modelling of the wind field	16
3.3. Estimations of wind field	19
3.4. Storm tide	20
4. AS/NZS 1170.2:2021 REGIONAL WIND SPEEDS	21
4.1. Comparison with design wind speed V_{500}	21
4.2. Implications of wind speeds for wind regions	23
4.2.1. Region D northern boundary	23
4.2.2. Region C south of 20° S	23
4.2.3. Region B	23
4.2.4. Region A	24
5. PERFORMANCE OF SOLAR PANELS	25
5.1. Undamaged solar panels	26
5.2. Ground-mounted inclined solar panels	27
5.2.1. Failure of the panels in bending	27
5.2.2. Tearing of the panel chassis in bolted connections	28
5.2.3. Failure of clamped connections	29
5.3. Inclined panels mounted on shipping containers	30

5.4. Roof-mounted solar panels parallel to building roofs	31
5.4.1. Failure of clamps between the chassis and the rails	32
5.4.2. Failure of the roofing fasteners	33
5.4.3. Structural damage to roofs under solar panels	34
5.5. Debris damage	34
5.6. Structural Design criteria for solar panels	36
6. PERFORMANCE OF SHEDS	37
6.1. Maintenance issues	38
6.2. Lightweight shed systems	40
6.3. Curved roofs	41
6.4. Racking failures	42
7. PERFORMANCE OF DONGAS	43
7.1. The capacity of prefabricated dongas	44
7.2. Capacity of donga anchorage	46
7.3. Verandas and other attachments to dongas	48
7.4. Maintenance issues	49
8. PERFORMANCE OF OTHER BUILDINGS	50
8.1. Resilient features	50
8.2. Roof sheeting to batten failure	51
8.3. Failure of batten to rafter or truss connections	52
8.4. Veranda failures	52
8.5. Roof-mounted items	53
8.6. Implications for buildings in remote communities	54

9. CONCLUSIONS	55
9.1. Wind field	55
9.2. Solar panels	55
9.3. Sheds	56
9.4. Dongas	56
9.5. Other buildings	57
10. RECOMMENDATIONS	58
11. REFERENCES	59

1. Introduction

1.1. Severe Tropical Cyclone Ilsa Overview

Severe Tropical Cyclone Ilsa (TC Ilsa) crossed the coast near Pardoo Roadhouse in the Pilbara region of Western Australia as a Category 5 system just before midnight on Thursday, 13 April 2023. Pardoo Roadhouse is around 130 km east of Port Hedland and is on the northern border of wind region D. Some fishermen who were at sea in the path of TC Ilsa were presumed drowned, but there was no reported loss of life on land.

Although TC Ilsa caused severe structural damage to the roadhouse, and some cattle station buildings, mainly sheds, and solar panels, and to solar pumps used on cattle watering points, its path was mainly over sparsely populated areas. No buildings in the area surveyed were damaged by the storm tide.

1.2. Purpose of the report

This report presents the outcomes of the joint Cyclone Testing Station (CTS), the Department of Mines, Industry Regulation and Safety, Building and Energy Division (Building and Energy), and the WA Department of Fire and Emergency Services (DFES) field investigation. The aim of the investigation was to establish the wind field of TC Ilsa and investigate damage to buildings in the affected area.

The report identifies problems in building performance and highlights some issues that need to be considered for changes to building practices, ongoing maintenance and Codes and Standards.

1.3. Investigation

The field study commenced on Wednesday, 26 April 2023 and concluded on Monday, 1 May 2023. The two-person investigation team included a representative from the CTS and one from Building and Energy. DFES provided data on damaged buildings and the contact details of people in the area.

Figure 1-1 shows the study area in yellow, with the path of the cyclone shown in white. The investigation team focused on determining the wind field using damage to road signs and vegetation. The team also assessed structural damage to solar panels, sheds and dongas.



Figure 1-1 Study area

2. Severe Tropical Cyclone Ilsa

2.1. Generation and predictions

The following information was provided by the Bureau of Meteorology:

“Severe Tropical Cyclone Ilsa crossed the east Pilbara coast at category 5 intensity just before midnight local time on Thursday 13 April 2023.

A tropical low that formed in the Timor Sea on 6 April moved southwest and developed slowly. It reached tropical cyclone intensity at 0600 UTC 11 April (1400 AWST 11 April, AWST = UTC+8 hours), about 400 km to the north northwest of Broome. During 11 April the environment became more favourable for development and the cyclone underwent rapid intensification. Ilsa reached severe Category 3 strength by 0000 UTC 12 April, only 18 hours after formation. The movement of Ilsa began to slow during 13 April and it turned south towards the Pilbara coast. Ilsa continued to intensify under favourable conditions and reached category 5 strength at 0600 UTC 13 April, some 180 kilometres to the north of Port Hedland.

Severe Tropical Cyclone Ilsa turned to the southeast from this point and accelerated towards the Pilbara coast, crossing near the Pardoo Roadhouse at 1600 UTC 13 April, around midnight local time, with a peak 10-minute mean wind intensity of 125 kn (230 km/h). Once the tropical cyclone crossed the coast and moved inland it began to weaken, decreasing below Category 3 intensity by 0600 UTC 14 April and then below tropical cyclone intensity by 1200 UTC 14 April over eastern parts of inland Western Australia.

Ilsa crossed the Pilbara coast in a relatively sparsely populated location; which limited the reported damage. However, the Pardoo Roadhouse and pastoral stations, including Pardoo and Warrawagine, sustained severe damage. Other communities along the track further inland such as Telfer, Punmu and Parnngurr experienced mostly minor building damage. Heavy rainfall was recorded along the track but no significant flooding was experienced.

Two Indonesian fishing boats were caught in the path of Ilsa off Rowley Shoals. One boat sank with at least nine fishermen feared drowned. The other boat ran aground at Bedwell Island on the northern end of Rowley Shoals. The eleven Indonesian fishermen survived six days without food and water before being rescued. Ilsa also had a destructive impact on bird colonies particularly the brown boobies and frigate birds on Bedout Island.

Ilsa passed directly over the Bureau of Meteorology's offshore observing sites at Rowley Shoals and Bedout Island as well as the inland site of Telfer. The peak 118 kn (219 km/h) 10-minute mean wind observation and the 155.9 kn (289 km/h) 3-sec wind gust at Bedout Island are the highest known recorded on a standard Bureau instrument. Although it is still significantly lower than the gust recorded on Barrow Island in Olivia.”

2.2. Track

Figure 2-1 shows the track of TC Ilsa provided by the Bureau of Meteorology.

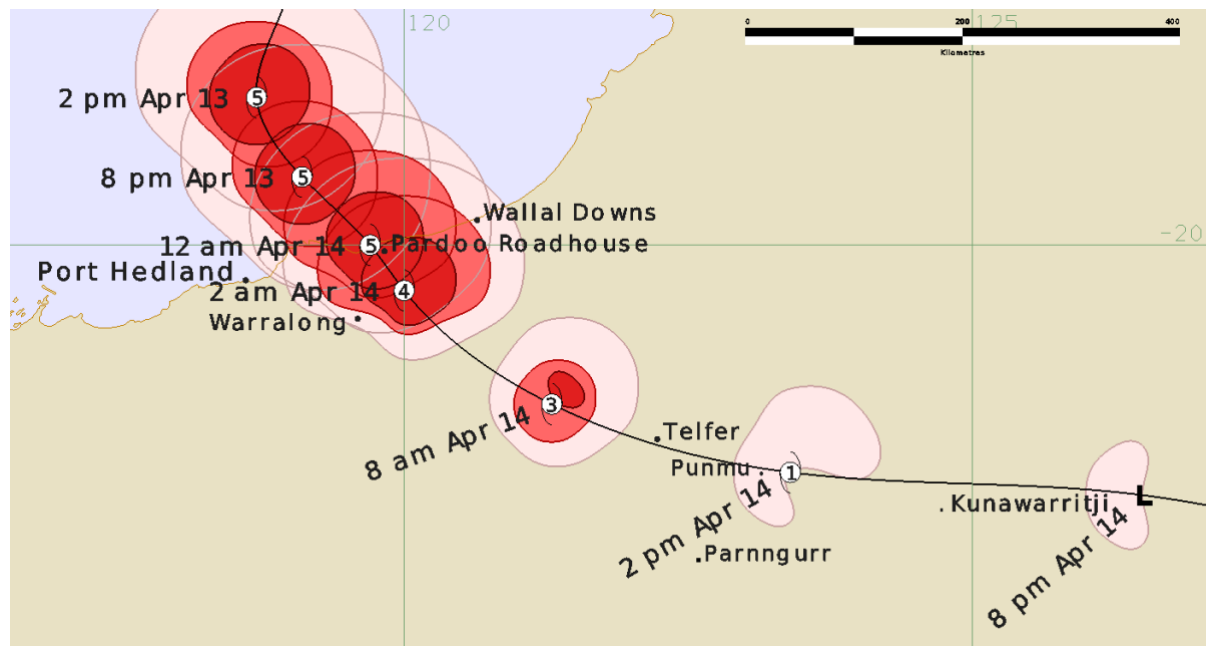


Figure 2-1 TC Ilsa track – Courtesy of BoM

2.3. Anemometer data

Figure 2-2 shows the wind speeds recorded at various locations before, during and after TC Ilsa crossed the coast. This data was downloaded from Bureau of Meteorology (BoM) Automatic Weather Stations (AWS) (Bureau of Meteorology, 2023). The anemometers at Rowley Shoals and Bedout Island experienced the eye of the cyclone but failed soon afterwards. The upper plot in Figure 2-2 shows the anemometer data referenced to Australian Western Standard Time (AWST), and the lower plot shows the recorded atmospheric pressure.

The anemometer data was recorded as 3-sec gusts. Rowley Shoals and Bedout Island were surrounded by ocean, but the other anemometers all had open country on the upwind approach. In correcting them for standard conditions, the $M_{z,cat}$ table was used to correct for Terrain Categories other than TC2. The relationship between gust duration and turbulence intensity (Holmes and Ginger, 2012) was used to correct the speed for gust duration. The corrections and the 0.2-sec wind gust in standard conditions are summarised in Table 2-1. Standard conditions refer to measurement in flat, open country at a height of 10 m with no shielding elements. This is often thought of as equivalent to terrain at airports. The 0.2-sec gust is used as the reference wind speed in AS/NZS 1170.2 (Standards Australia, 2021).

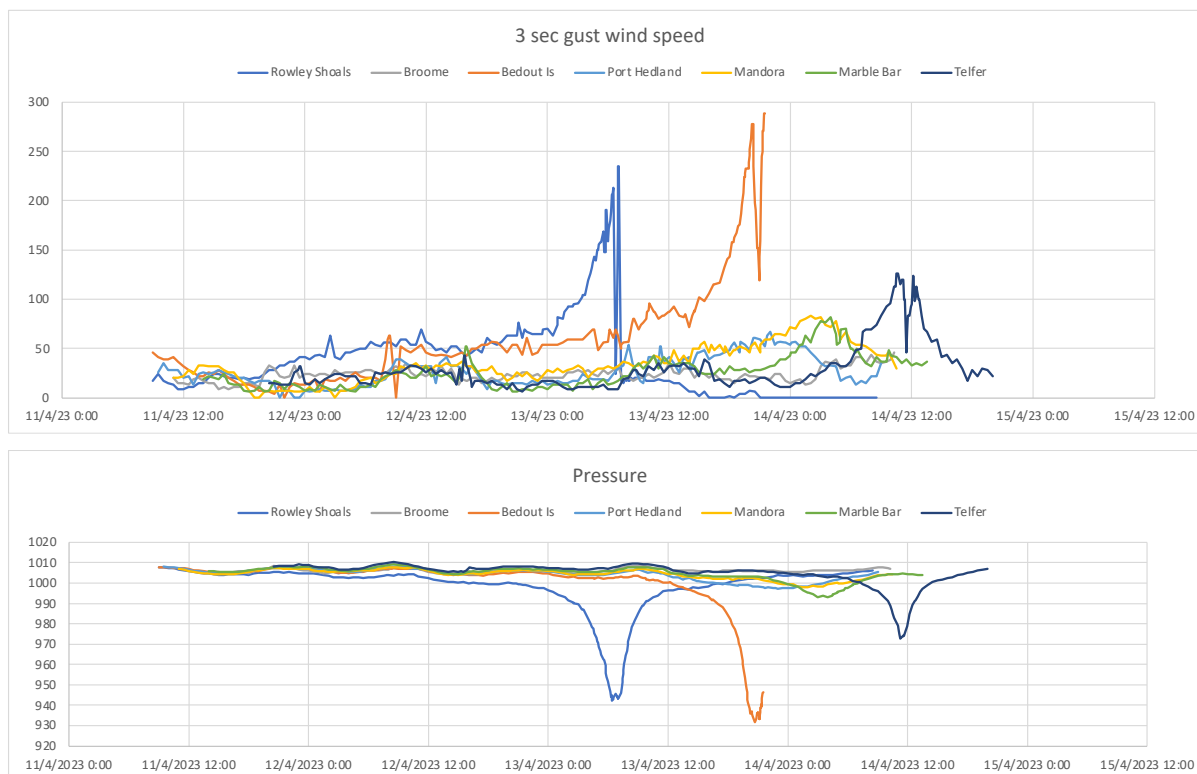


Figure 2-2 Wind speeds at different locations (Anemometer data from BoM website)

Table 2-1 Corrections to peak gust from AWS data

Station	Lowest pressure (hPa)	Time of max gust	max 3-sec gust (kph)	Dirn	3-sec gust (m/s)	TC	0.2-sec gust (m/s)	0.2-sec gust corrected for $M_{z,cat}$ (m/s)
Rowley Shoals	942.3	13/4/2023 7:02	235	NNW	65.3	1	72.2	66.8
Bedout Is	931.7	13/4/2023 20:22	289	SW	80.3	1	89.4	82.7
Broome	1004.3	13/4/2023 15:00	46	NNW	12.8	2	14.2	14.2
Mandora	998.1	14/4/2023 2:00	83	N	23.1	2	25.8	25.8
Port Hedland	997.2	13/4/2023 22:00	67	S	18.6	2	20.7	20.7
Marble Bar	993	14/4/2023 4:00	82	SSE	22.8	2	25.5	25.5
Telfer	972.7	14/4/2023 10:37	126	ENE	35.0	2	39.4	39.4

The anemometer data were used as the primary reference for wind speed calculations. Other methods of estimating wind speeds to interpolate wind speeds between the anemometers across the whole study area are presented in Section 3.

3. Estimating the TC Ilsa wind field

The wind field in TC Ilsa was estimated using a combination of techniques:

- Converting anemometer records to 0.2-sec gusts relative to standard conditions to compare with design wind velocities for the same location.
- Modelling the cyclone wind speeds using the Holland model, the identified track, size and pressure characteristics of TC Ilsa.
- Measuring road signs to obtain upper bound estimates (where the sign was still standing) and lower bound estimates (where the sign had failed by permanently bending the pole(s)).
- Establishing rough wind speed contours by identifying locations with similar vegetation damage (focusing on one tree species because different species have different strengths).
- Confirming wind directions from damage to trees, termite mounds, and damaged structures.
- Identifying the location of the eye using observations from residents.

Section 2.3 outlined the examination of the anemometer data. Section 3.1 discusses the ground-truthing techniques, and Section 3.2 outlines the numerical modelling of the wind speed.

3.1. Field investigation

The field investigation aimed to confirm the tropical cyclone's track and provide input to wind speed estimations.

3.1.1. TC Ilsa track

Vegetation damage was used to indicate wind direction. Light vegetation, such as wattles, broke off near ground level or was permanently bent. This type of vegetation grew in most locations visited during the investigation and provided a good indication of wind direction. In some cases, evidence of wind from two or more directions was noted. Figure 3-1 shows an example of wind-blown light vegetation with the predominant wind from left-to-right.



Figure 3-1 Light scrub blown from left to right

The relatively straight, white-bark river gums were selected as the standard vegetation for assessment of wind, as they were found near rivers, seasonal creeks and floodways that were located throughout the study area. Figure 3-2 shows damage to river gums. The extent of damage to river gums was used to indicate wind speed contour lines, and the direction of fall of the damaged parts of the trees was used to estimate wind direction in some cases.



Figure 3-2 River gums damaged by wind

Termite mounds could also give an estimation of wind direction in desert regions. Gravel and sand lifted from the ground by the wind eroded the mounds on the sides from which the wind had been blowing. Figure 3-3 shows a termite mound where the wind had been from the East and had caused erosion on the left side of the mound. The photo on the left indicates that the erosion had exposed galleries and chambers inside the mound.



Figure 3-3 Erosion of termite mound by wind, rain and sand

In addition, where structures had been damaged, the wind direction could be inferred from the direction of travel of the detached elements or by the direction of fall of tall elements such as the power transmission tower shown in Figure 3-4. This part of the line had been decommissioned but the conductors were in place prior to TC Ilsa.



Figure 3-4 Damage to power transmission tower

Maps of the principal wind directions, representing the first 350 km of the cyclone track over land, were constructed using observations from a vehicle and the ground-truthing techniques described above. The plot of wind directions helped refine the cyclone track. It was possible to estimate the time and duration of the passage of the eye from discussions with people who had sheltered on their properties during the cyclone. In some cases, security camera vision enabled estimates of the duration of the eye and evaluation of the wind directions before and after the eye.

The ground-truthing indicated that the eye passed between Pardoo Station and Pardoo Roadhouse, over Yarrie Station and the Yarrie Mine Village, over Warrawagine Station and Telfer Mine Village. The refined path is presented in Figure 3-7.

3.1.2. Evaluation of road signs

Upper and lower-bound wind speeds were estimated using damage to 51 road signs along the path of TC Ilsa.

- Lower-bound signs were those which had failed by bending the posts (forming 'plastic hinges'). The wind speed to cause the damage was higher than the wind speed that would have created enough load to fail the post, and this is shown in the left-hand photo of Figure 3-5.
- Upper-bound signs had not failed by forming plastic hinges in the posts and remained upright. The wind speed cannot have exceeded the speed that would have created enough load to fail the post, shown in the middle photo of Figure 3-5.
- Where the pole had just started to fail but hadn't developed a full plastic hinge, the lower-bound wind speed was likely close to the actual wind speed. This is shown in the right-hand photo of Figure 3-5. Note that sand had blasted most of the paint off the surface of this sign.



Figure 3-5 Lower-bound and upper-bound road signs

The coordinates of each sign were collected along with the principal wind direction at the sign, the dimensions, the characteristics and size of the post, and the distance between the signs and the plastic hinge. Signs were only used if the wind was within 45 degrees of being perpendicular to the sign, there was no upwind shielding of the sign, and there was no trace of debris damage that may have indicated

that the damage was inflicted by large debris and not by wind. Information was collected on the terrain and topography in the direction from which the wind blew to cause the damage.

The information from each sign was used to calculate a lower or upper bound of the wind speed at that location, and the wind speed information was plotted as shown in Figure 3-6. The black line in Figure 3-6 is the estimated path of the cyclone. There were four locations where nearby lower- and upper-bound signs converged on a single wind speed (highlighted by red circles). The wind speeds at those locations, and the anemometer data from the Bureau of Meteorology automatic weather stations were used to prepare a preliminary estimate of the wind speed field.

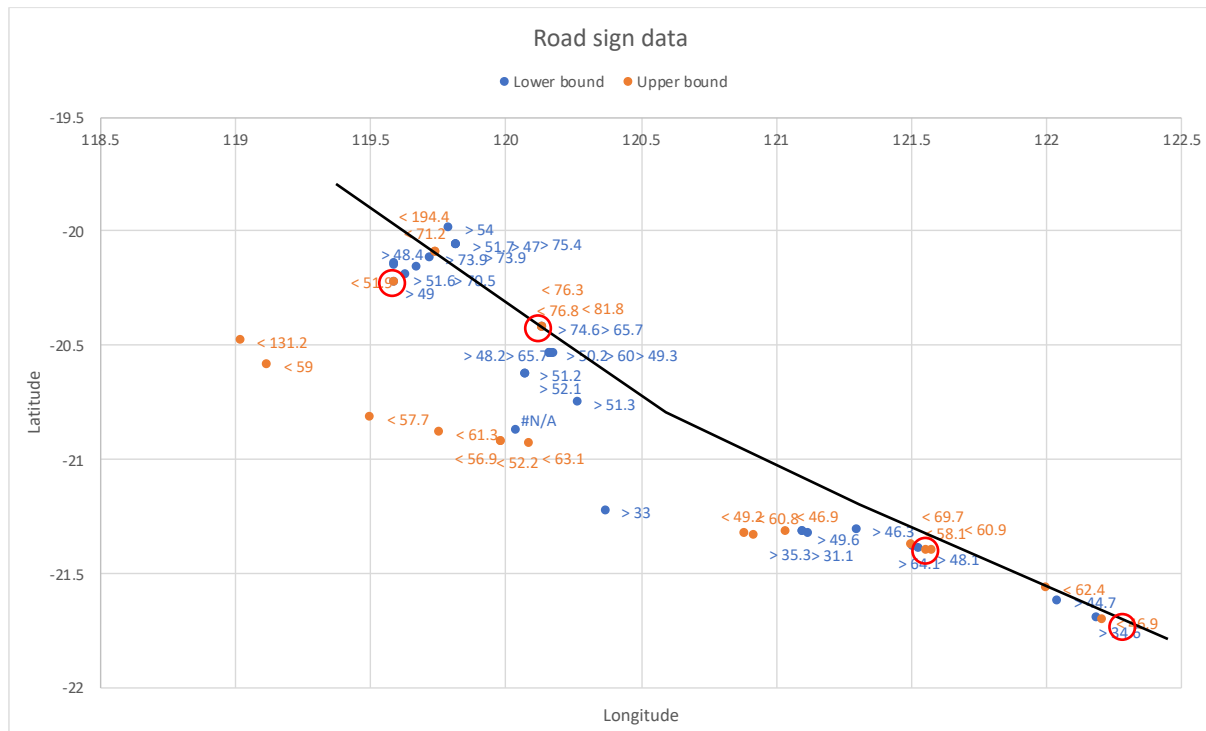


Figure 3-6 Summary information from road signs

In addition, the observations of river gum damage illustrated in Figure 3-2 noted the following attributes:

- In lower wind speed areas, the extent and location of leaf cover remaining
- In higher wind speed areas, the diameter of branches or trunks that had been broken.

This qualitative information was used to draft the shape of wind speed contours on the map. The shape of the contours, the road sign data and the anemometer data gave a map of wind speeds over the study area. This was combined with the map from the numerical model indicated in Section 3.2 to provide the final wind field.

3.2. Numerical modelling of the wind field

The Australia-wide version of the SEAtide model (SEA, 2020) was used to both forecast and hindcast the storm tide response of TC Ilsa, and the wind and surface pressure swath was calibrated using the available AWS sites (BoM and Department of Primary Industries and Regional Development). The BoM preliminary analysis track based on the Port Hedland radar (Joe Courtney, pers. comm.) provided the base reference for an estimated minimum central pressure (MSLP) and V_{max} (V 10-min). The track positions after landfall were adjusted to match cyclone eye location from the ground-truth techniques and to reflect recorded wind direction changes at Telfer, which experienced the full eye. Figure 3-7

shows the original BoM track in yellow and the final track after adjustments in red. Minor adjustments were also made to some BoM-estimated radius of maximum winds (R_{max}) values.

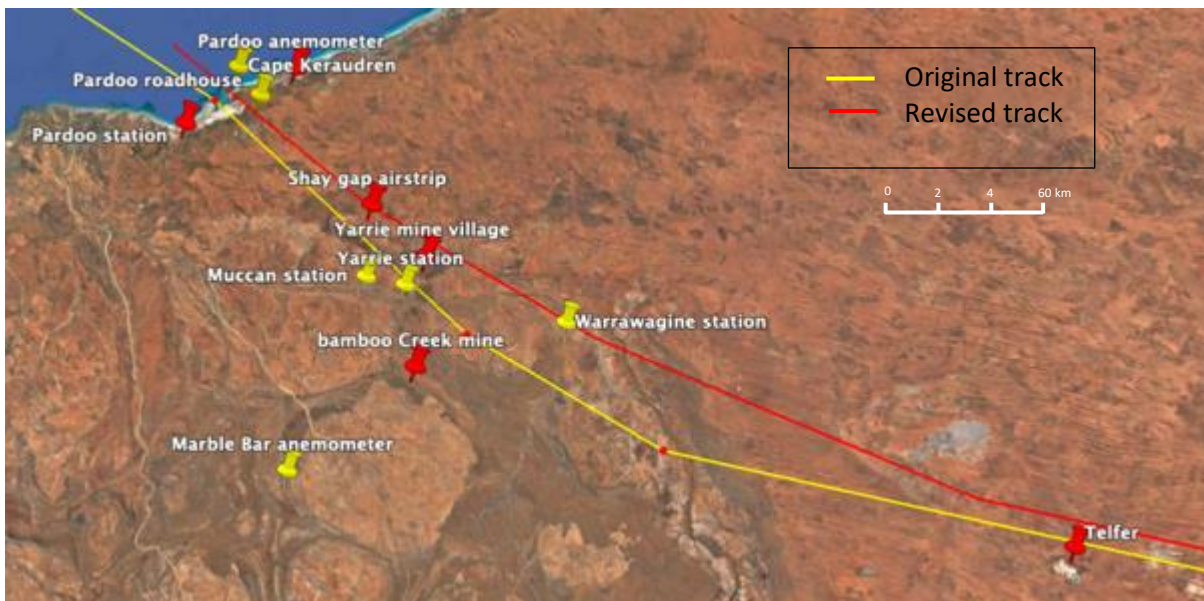


Figure 3-7 Adjustment of TC Ilsa track

The input parameters are summarised in Figure 3-8. It shows the track and the radius of maximum winds used at several locations. The calm of the eye was a few kilometres inside the radius of maximum winds shown.

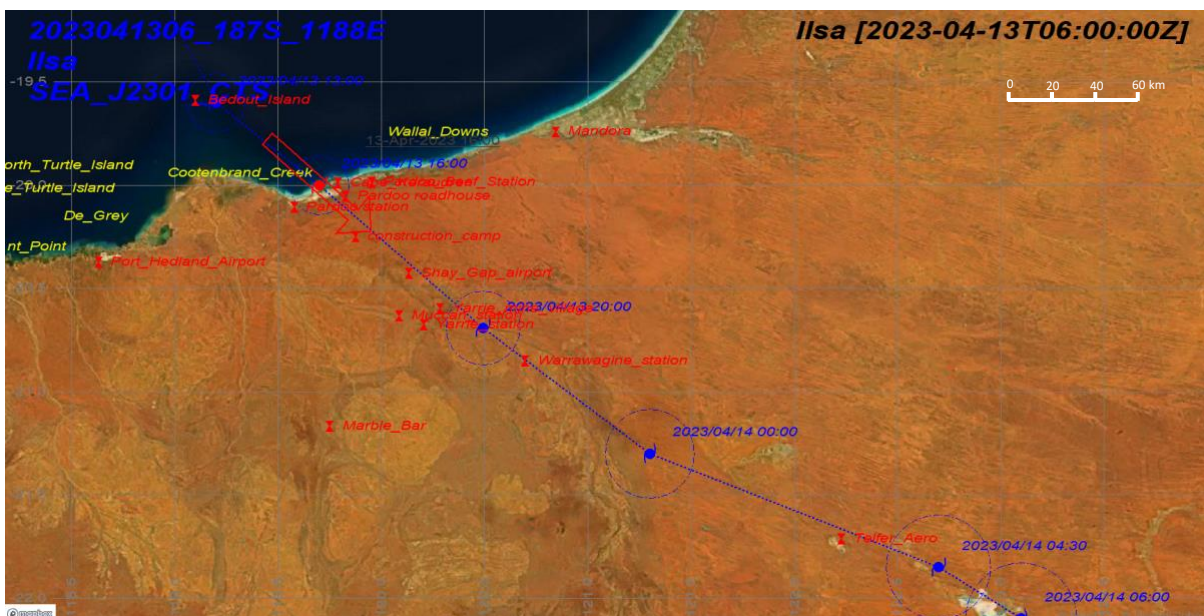


Figure 3-8 TC Ilsa modelling details

SEAtide uses a 'double Holland' parametric wind and pressure formulation that can adjust the storm structure to accommodate expected changes at landfall as the inner core typically tends to decay and expand as the surface energy flux decreases. The model can present results in various surface wind units, averaging periods, and roughness categories. The measured AWS pressures, V 10-min mean winds and V 3-sec gusts were used for calibration, while the modelled results for V 0.2-sec peak gusts in Terrain Category 2 at 10 m height (standard conditions) as used in AS/NZS 1170.2 (Standards Australia, 2021) have been used for comparison with observed building damage.

The anemometer data at a few AWS were compared with the output of the model to calibrate it. Figure 3-9 shows that the predicted 10-min mean wind speed, the 3-sec peak gust speed and the mean wind direction output from the model match the AWS data from Telfer well. The lines represent the model data, and the points are taken from the Bureau of Meteorology AWS data.

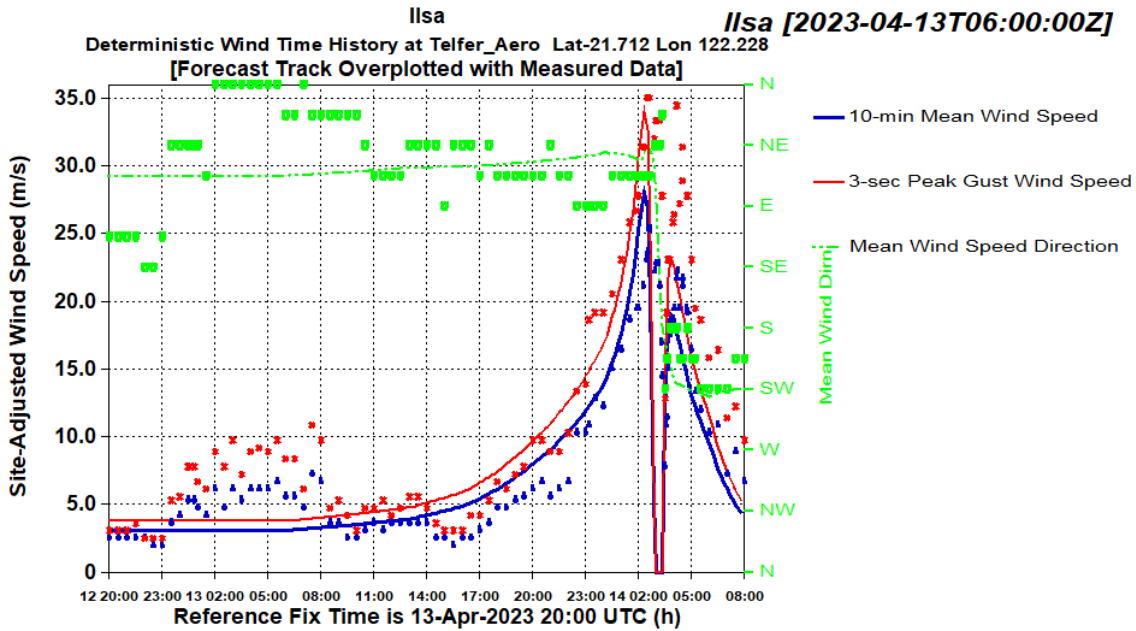


Figure 3-9 Matching model output with AWS data at Telfer

The envelope of maximum wind speeds and directions is illustrated in Figure 3-10. An envelope data file that gave wind speed at around 2.5 minute (0° 2.5') intervals for both latitude and longitude was produced. This data were used to construct the wind speed map shown in Figure 3-11.

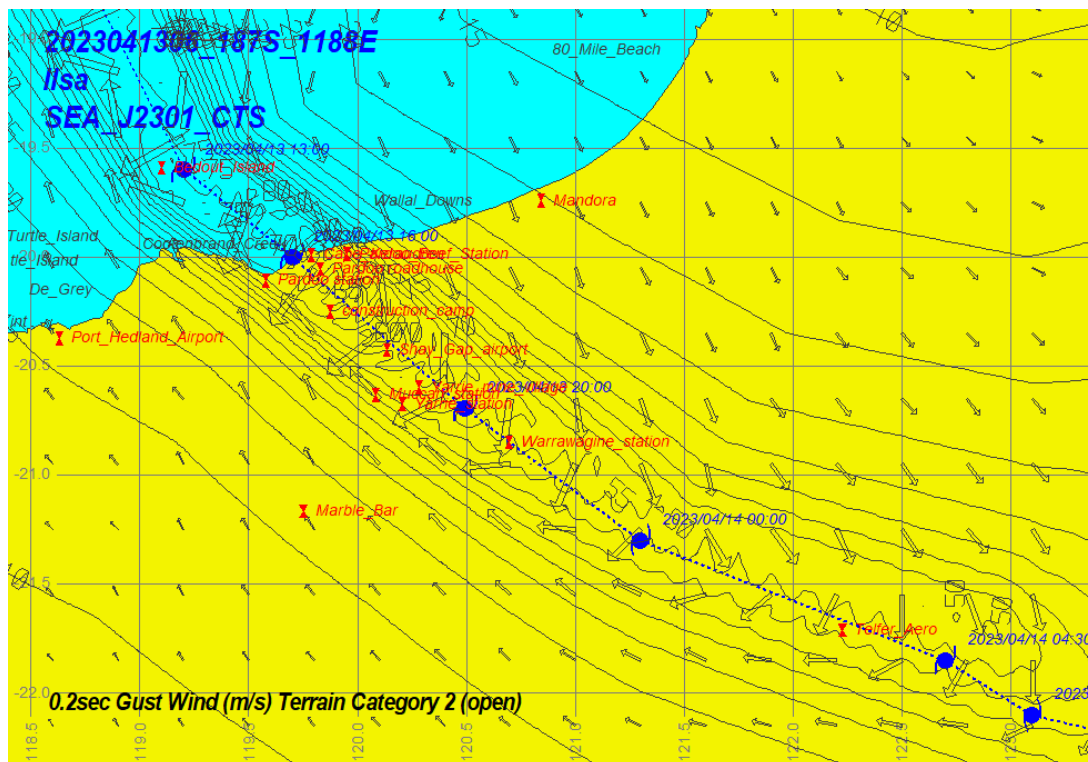


Figure 3-10 Summary of numerical model output

The peak modelled storm tide at the isolated coastline north of landfall was estimated to only exceed HAT (Highest Astronomical Tide) levels by up to 1 m along a distance of about 25 km, despite the peak surge component being around 6 m. This was due to the locally high tidal range and the timing of landfall near a low tide. However, even modest exceedance of HAT in areas with salt pan margins, such as near Pardoo, would have experienced shallow saltwater incursion several kilometres inland during the extreme onshore winds. There are no tide gauges along this section of the coastline.

3.3. Estimations of wind field

The amalgamation of the numerical model and the field data gave the wind field shown in Figure 3-11 with the velocities presented as 0.2 -sec gusts in standard conditions and directly comparable with V_R in AS/NZS 1170.2 (Standards Australia, 2021).

Figure 3-11 shows that winds at sea exceeded 80 m/s, and parts of the coastal strip in wind regions C and D near the crossing point experienced winds over 80 m/s. This included facilities at Cape Keraudren and the Pardoo Roadhouse.

The peak wind speeds were more than 70 m/s as the cyclone crossed into wind region C and over 60 m/s as it crossed into wind region B. The wind speeds were over 50 m/s as the cyclone crossed into wind region A. The estimated maximum 0.2-sec gust wind speeds (referencing standard conditions) at key locations are summarised in Table 3-1.

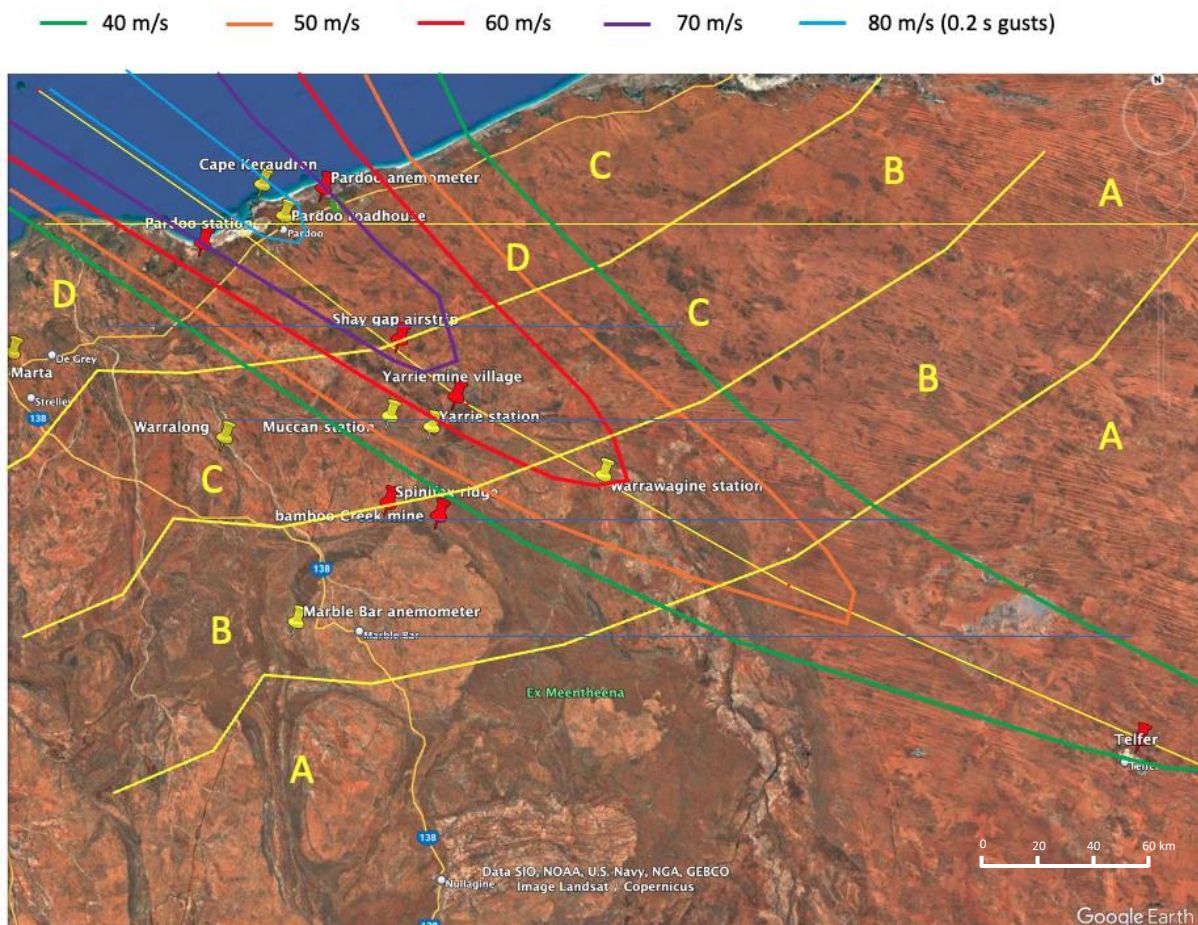


Figure 3-11 Wind field estimate TC Ilsa

Figure 3-11 shows wind regions from AS/NZS 1170.2, which has a discontinuity at 20° S. South of this latitude the coastal strip is wind region D with a progression inland through wind regions C, B and A. However north of 20° S, the coastal strip is wind region C. The wind field shown penetrated all wind regions south of 20° S, but only wind region C, north of 20° S.

Table 3-1 Estimates of 0.2-sec standard conditions wind speed

Location	Wind speed V 0.2-sec (kph)	Wind speed V 0.2-sec (m/s)
Cape Keraudren	297	82
Pardoo Roadhouse	287	80
Pardoo station	255	71
Pardoo anemometer	287	80
Jinparinya	64	18
Shay Gap airport	248	69
Yarrie Mine village	224	62
Yarrie station	201	56
Muccan station	196	54
Warrawagine station	212	59
Bamboo Ck Mine	114	32
Telfer	142	39
Marble Bar	92	25

3.4. Storm tide

Few areas along the coast near the crossing were easily accessible by road. However, permission was obtained to access Cape Keraudren to estimate the height of the storm tide. The foreshore was accessed to look for signs indicating the maximum height of the storm tide. Figure 3-12 shows the beach on the east side of Cape Keraudren. The observations were repeated at two locations on the west side of the Cape. Figure 3-12 shows:

- Wave erosion of the base of the dunes.
- The upper extent of the seagrass debris was at the foot of the dunes.

Also, there was no sign of exit channels excavated by the retreating seawater in the car park, which was only just above the base of the dunes. If the car park had been flooded, then the water exiting the wide, flat area of the car park would have created channels. The absence of these channels in the sand between the car park and the beach indicates that the car park had not been inundated by seawater. The highest level likely attained by the storm tide was the base of the dunes – close to the Highest Astronomical Tide. This is a similar conclusion to that presented in Section 3.2 as part of the numerical modelling of TC Ilsa.



Figure 3-12 Observations of storm tide height

4. AS/NZS 1170.2:2021 Regional wind speeds

Figure 3-11 shows the estimated wind speed contours as 0.2-sec gust wind speed in standard conditions. It also shows the wind regions from AS/NZS 1170.2:2021 (Standards Australia 2021). The crossing point was right on the northern-most point of wind region D. The region of maximum winds just north of the track encroached on wind region C. This section presents a comparison of the estimated wind speeds with the regional wind velocities presented in AS/NZS 1170.2:2021. This report makes no assessment or estimate of the annual exceedance probability of STC Ilsa but compares the cyclone's estimated wind speeds to the design wind speeds detailed in AS/NZS1170.2:2021.

4.1. Comparison with design wind speed V_{500}

The estimated 0.2-sec gust wind speeds from Table 3-1 were compared with the design level for the same location. The distance from the smoothed coastline was estimated as the shortest direct distance from the location to the smoothed coastline. In wind regions D and C, the design wind speed was interpolated between the wind speed at the coast-side and inland boundaries in the region as indicated in AS/NZS 1170.2:2021.

The TC Ilsa wind speed was divided by the design wind speed at the V_{500} level, which gave a ratio for many locations around 100%. The last four lines of the table present the peak wind speed at each wind region boundary as calculated from the numerical wind field. Wind region C is a special case, as TC Ilsa crossed the coast at the northern boundary of wind region D. Table 4-1 presents the wind speed where the peak speed zone enters the wind region C boundary 50 km inland from the coast (around the Shay Gap airport). The effects of the wind region C/D boundary at 20° latitude are discussed in Section 4.2.1.

Table 4-1 Comparison of TC Ilsa 0.2-sec gust speed with V_{500} in AS/NZS 1170.2:2021

Location	0.2-sec Wind speed (kph)	0.2-sec Wind speed (m/s)	Wind region	Distance from coast (km)	Design V_{500} (m/s)	0.2-sec wind speed / V_{500} (%)
Cape Keraudren	297	82	D	0	80	103%
Pardoo Roadhouse	287	80	D	13	76	104%
Pardoo station	255	71	D	5	79	90%
Pardoo anemometer	287	80	D	4	79	101%
Jinparinya	64	18	D	10	77	23%
Shay Gap airport	248	69	C	54	65	106%
Yarrie Mine village	224	62	C	77	61	102%
Yarrie station	201	56	C	85	60	93%
Muccan station	196	54	C	77	61	89%
Warrawagine station	212	59	B2	116	57	103%
Bamboo Ck Mine	114	32	B2	110	57	56%
Marble Bar	92	25	B2	130	57	45%
Telfer	142	39	A	268	45	87%
Wind region D	297	82	D	0	80	103%
Wind region C (south of 20° S)	259	72	C	50	66	109%
Wind region B2	228	63	B2	100	57	111%
Wind region A	198	55	A	150	45	122%

Figure 4-1 was generated using the 0.2-sec gust wind speed plot in Figure 3-11 and the design wind speeds tabulated for V_{500} in AS/NZS 1170.2 (Standards Australia, 2021). The design wind speeds were interpolated within wind regions C and D.

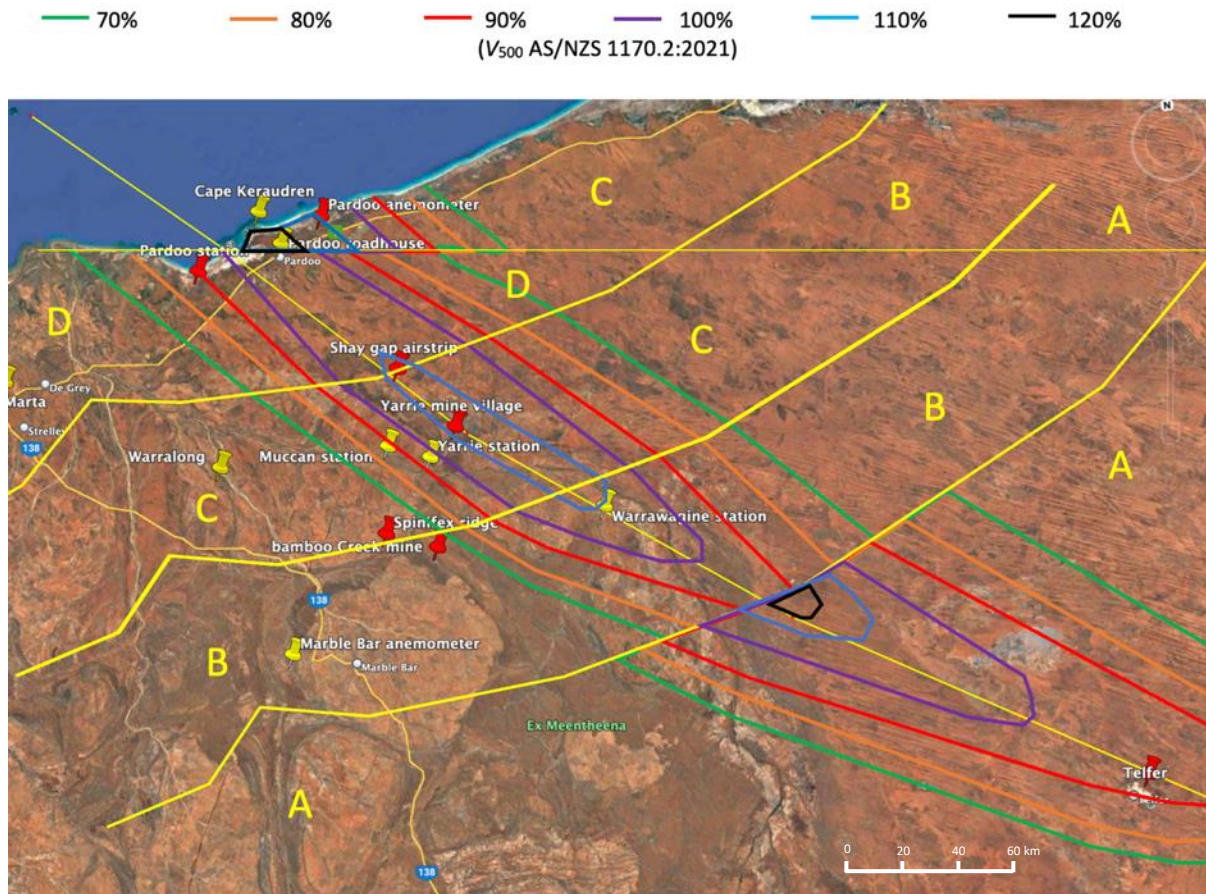


Figure 4-1 Percentage of design V_{500} experienced during TC Ilsa

The $V_{0.2}$ -sec gust wind speed estimated in TC Ilsa was plotted against the distance from the crossing point in Figure 4-2. It shows a gradual decrease with the distance covered overland. The plots show a dashed red line representing the reduction in design wind speed north of 20° S.

The left plot in Figure 4-2 shows the wind speed profile along the TC Ilsa track. Because the track was not normal (perpendicular) to the coastline, it travelled through wind region D for 60 km, wind region C for 61 km and wind region B for 62 km. This plot shows that the estimated peak TC Ilsa wind speed was higher than the V_{500} design wind speed for all but a short distance in region B near the region A boundary and in region A beyond 270 km from the coast. This is compatible with the extent of the 100% contour in Figure 4-1.

However, if the track had been normal to the coastline, it would have spent only 50 km in each zone. Assuming that the decay rate remained the same, this means it would have had a slightly higher wind speed when it crossed into each of wind regions C, B and A. This is shown in the right plot in Figure 4-2.

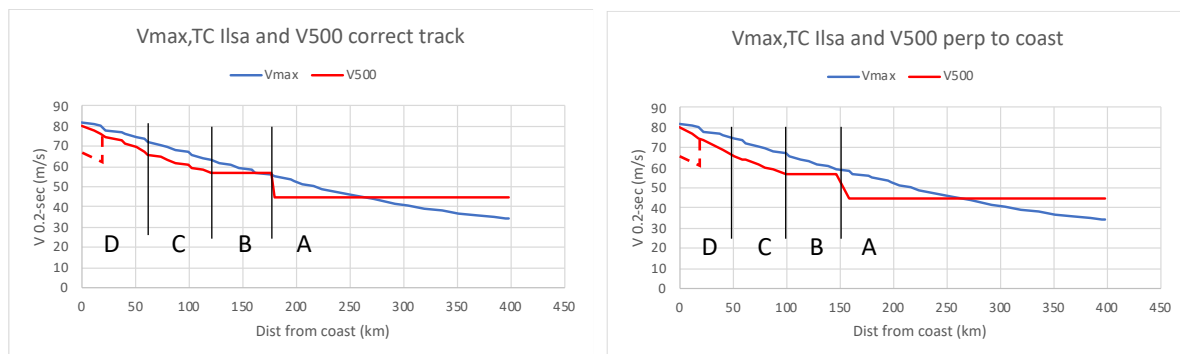


Figure 4-2 Plot of V 0.2-sec along the track of TC Ilsa

The actual wind speed profile shown on the left of Figure 4-2 and the notional profile had the path been perpendicular to the coast (the right hand plot in Figure 4-2), are only slightly different. Both plots show that the maximum 0.2-sec gust in standard conditions for most of the profile was higher than the design V_{500} .

4.2. Implications of wind speeds for wind regions

As indicated above, no assessment or estimate of the annual exceedance probability of STC Ilsa was made, but this section compares the estimated wind speeds to the design wind speeds detailed in AS/NZS1170.2:2021 to address relative differences across the study area.

4.2.1. Region D northern boundary

In a statistical study of the occurrence of severe tropical cyclones in WA, Holmes (2021) indicated that consideration should be given to extending the northern boundary of region D to the north by 1 or 2 degrees based on the number of observed impacts of severe storms north of 20° S. A proposal is currently being discussed by the Standards Australia committee that oversees AS/NZS 1170.2:2021 to amend the wind region D northern and southern boundaries.

Figure 4-1 shows the track crossed the Pilbara coast at the wind region C/D boundary (20° S). The numerical model indicated that maximum wind speeds on the eastern side of the eye were a little higher than those on the western side of the eye, which was confirmed in the field investigation. However, the coastal strip on the eastern side of the eye was in wind region C and the coastal strip on the western side of the eye was in wind region D. This meant that the strongest overland wind gusts were in wind region C, not wind region D. The maximum wind gusts in the region north of 20° S were more than 124% of the design wind speed (V_{500}). In comparison, those south of 20° S were around 100% of V_{500} . If wind region D extended north of 20° S, the maximum wind gusts near the coast would have been about 100% of V_{500} for wind region D, and there would not have been steps in the percentage of V_{500} plot at 20° S as shown in Figure 4-1. Even if TC Ilsa was an extremely rare event with a 1/10,000 Annual Exceedance Probability (AEP), the design wind speed with that AEP in wind region C just north of 20°S would still not have exceeded the estimated wind speed in the affected area.

4.2.2. Region C south of 20° S

The interpolation of wind speeds in regions D and C meant there was continuity of wind speed across both the coast-ward and the inland boundaries of wind region C south of 20° S. The peak 0.2-sec wind speeds in this part of wind region C during TC Ilsa were around 110% of V_{500} over a small area.

4.2.3. Region B

Figure 4-1 shows that a small area near the wind region B/C boundary experienced around 110% of V_{500} , but as there is no interpolation of the AS/NZS 1170.2 (Standards Australia, 2021) design wind speed in region B, the peak 0.2-sec gust decreased to a value less than V_{500} at the wind region A boundary.

The winds in wind region B resulted in broken windows and doors that gave high internal pressure to some buildings, but many had already been designed using appropriate internal pressures for large openings on one wall. A proposal is currently being discussed by the Standards Australia committee that oversees AS/NZS 1170.2:2021 to amend the design internal pressures for enclosed buildings in wind region B2. All wind region B in WA is wind region B2, so the amendment is relevant to buildings in the part of wind region B affected by TC Ilsa. Note that high internal pressure is already required in WA parts of wind region B in State Variations of NCC 2022 (Australian Building Codes Board, 2022).

4.2.4. Region A

The left-hand plot in Figure 4-2 shows that for 100 km inland of the wind region A boundary, the peak 0.2-sec wind speed was more than the relevant V_{500} . There were no buildings in the area of wind region A that experienced 0.2-sec wind gusts of 120% or more of V_{500} . However, elsewhere within wind region A, wind pressure or small debris created openings in the building envelope (photo on the left in Figure 4-3). The photo on the right shows an opening formed on a leeward surface of a building in wind region A.



Figure 4-3 Openings created in wind region A

Fortunately, both buildings illustrated in Figure 4-3 had been built to withstand high internal pressure, and the structural damage progressed no further. However, there is currently no requirement to design buildings in wind region A for high internal pressure.

5. Performance of Solar Panels

The investigation team examined solar panels on installations throughout the study area, including panels powering watering points on cattle stations; roof-mounted panels on sheds and houses; inclined arrays mounted on the ground and shipping containers; and a tracking panel array. Grid energy is unavailable in the study area, so solar panels are used extensively. The team was interested in examining the performance of solar panel systems under high wind conditions because this technology will be used more extensively in all parts of the country as Australia transitions to a sustainable energy environment.

The following terminology is used in this section:

Array – a group of panels that effectively presents a single surface

Panel – a glass-mounted photovoltaic element with a metal chassis. This is a single manufactured unit that is fixed into position to become part of an array.

Chassis – the rectangular metal frame that contains the glass-mounted photovoltaic element. This term is used to differentiate the chassis from a structural frame that may support several panels.

Upward-facing – the face of the panel that faces the sun to generate electricity

Downward-facing – the lower face of a panel

Ground-mounted – inclined arrays mounted on a structural frame that is directly in contact with the ground (see Figure 5-4)

Container-mounted – inclined arrays mounted on a structural frame that is attached to a shipping container (see Figure 5-10)

Roof-mounted – arrays fixed parallel to the roof (see Figure 5-15). No roof-mounted panels mounted on an inclined structural frame were observed in this study. The term in this report refers only to arrays fixed to rails parallel to the roof and within about 200 mm of the roof cladding.

Tracking panels – motorised panel support systems that rotate the panels so that the panel surface remains in an orientation favourable to generating electricity as the sun moves across the sky (see Figure 5-2).

Figure 5-1 shows the location of all types of larger solar arrays (ground-mounted, container-mounted, and roof-mounted) observed during the investigation. Red dots indicate locations of damaged systems, and green dots indicate the location of systems that remained functional. (There were a number of different systems in some of the locations marked.) The wind velocities in Figure 5-1 refer to speeds equivalent to 0.2-sec gusts at a height of 10 m in terrain category 2 (0.2-sec standard condition gusts).

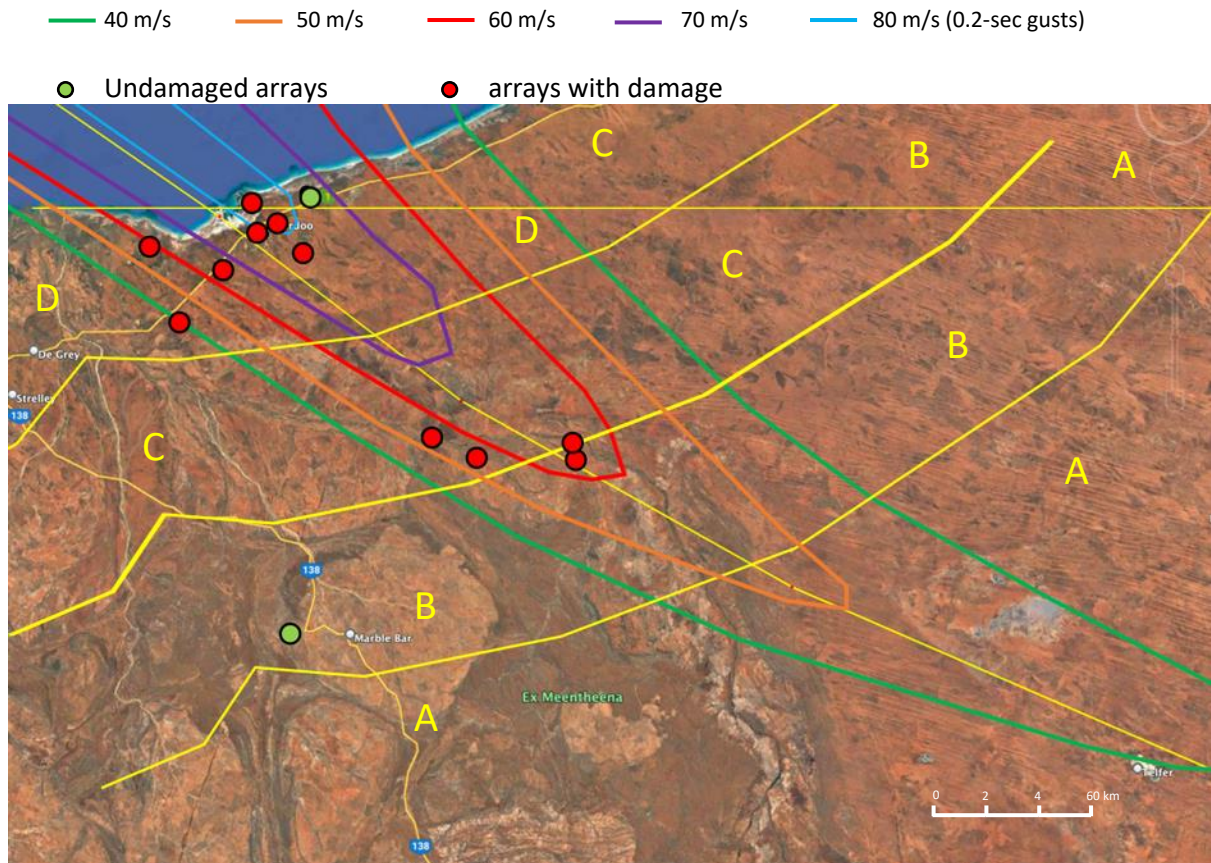


Figure 5-1 Location of solar panels observed in the study area

5.1. Undamaged solar panels

The tracking panels for the town power supply at Marble Bar were undamaged and functional during and after the event, as shown in Figure 5-2. The maximum peak 0.2-sec standard condition gust wind speed at the Marble Bar AWS was estimated at only 25 m/s.



Figure 5-2 Tracking solar array Marble Bar

Figure 5-3 shows a ground-mounted fixed array that experienced 0.2-sec standard condition gusts of around 70 m/s. The highest wind was towards the upward-facing slope, as shown by the blue arrow. There was no sign of bending failures or detachment of the panels. There were few obstructions upwind of the installation that would have introduced extra turbulence or become wind-borne debris if they had failed. Although gravel was on the ground around the panels, the glass had not been broken. The precise details of the mounting system were not observed elsewhere in this study – the clamps were fixed directly to the rails.



Figure 5-3 Undamaged ground-mounted solar arrays

5.2. Ground-mounted inclined solar panels

Ground-mounted inclined solar panel arrays are used extensively in remote communities in the Pilbara as there is no grid energy available.

5.2.1. Failure of the panels in bending

Several inclined panels showed bending failures of the panel itself. Where the wind was towards the upward-facing slope of the panels, they failed by bending inwards, and where the wind was towards the downward-facing slope of the panels, they failed upwards. Inward failures are shown in Figure 5-4, and an upward failure is shown in Figure 5-5. The downward failures in the left-hand photo of Figure 5-4 were observed where the peak 0.2-sec standard condition gust exceeded 80 m/s, and in the right-hand photo, the 0.2-sec standard gust exceeded 55 m/s. As Figure 5-3 shows, some other brands of panels could resist wind gusts of 70 m/s without the glass failing in bending.



Figure 5-4 Examples of failure of panels due to wind pressure on the upward-facing slope of the panel (net +ve pressure)

The movement of the panel shown in the left-hand photo of Figure 5-5 was sufficient for it to disengage from the chassis at the base. The chassis remains (photo on the right), but the panel has bowed outward enough to be removed entirely. In this case, the chassis was directly fixed to the rails by bolts – highlighted by the circle.



Figure 5-5 Failure of the panel due to wind pressure on the downward-facing slope of the panel (net -ve pressure)

In some cases, all the panels failed under the action of the wind pressure and in others, just one panel failed. Because the location of the failed panels did not appear to be associated with the location of the highest net pressures on the array, it appears that specific details of each individual panel supplied (such as the characteristics of the glass in the panel and/or its connection with the chassis) contributed to the level of performance achieved. The high variability of the performance of the panels indicated high variability in the characteristics of the panels.

Recommendation

Test glass in solar panel systems using methods that replicate the fluctuating nature of wind loads.

5.2.2. Tearing of the panel chassis in bolted connections

Some panels were bolted to a clip through the back of the chassis, and some of them failed by tearing through the thin chassis metal. Under cyclonic loads, the forces on the panels are repeated, and low-cycle metal fatigue may have played a role in the tear-out failure. The photo on the left of Figure 5-6 shows an example of a clip connection that hadn't failed. In other cases, the bolt tore through the chassis and left a small portion of the chassis under the spring washer, as shown in the inset. The photo on the right of Figure 5-6 shows some bolted fastenings left in the frame after they had torn out of the chassis on a directly bolted connection.



Figure 5-6 Panels in which the chassis tore at the fastenings

5.2.3. Failure of clamped connections

Some inclined solar systems use clamps between the upper surface of the panel chassis and the extruded aluminium frame underneath. Many of these systems, such as the one shown in Figure 5-3, performed well, but in other cases, the clamps either broke, as shown in Figure 5-7, came loose, or were not tightened correctly when installed. Figure 5-8 shows clamps that had not broken but had released the panels. The broken clamp shown in Figure 5-7 may have occurred on a panel that had been partially released by the other clamps. Fluctuating loads may have affected the performance of the clamps and the strength of the chassis at the bolts.

Recommendation

Test solar panel systems using methods that replicate the fluctuating nature of wind loads.



Figure 5-7 Broken clamps



Figure 5-8 Clamps that have released the panels

The left-hand photo in Figure 5-9 shows a panel that had been clamped to an inclined ground-mounted frame but was released by the clamps. The panel had moved more than 100 m from its original location and had sustained damage as it bounced across the ground. The right-hand photo shows a cattle watering point with clips missing from the array.



Figure 5-9 Previously clamped panel that has been released from the frame

5.3. Inclined panels mounted on shipping containers

Several solar arrays had been mounted on inclined frames fixed to shipping containers. The shipping containers contained batteries and other electronic equipment to produce an independent power supply. The shipping containers were all securely anchored to large concrete blocks.

The failure modes discussed in Section 5.2 also applied to panels mounted on shipping containers. Figure 5-10 shows some failures of solar panel arrays mounted on shipping containers with the wind direction that caused the failure indicated by blue arrows. In some cases, the panels had been damaged by wind directed at the upward facing side of the panels, but in one case, the failures were caused by wind onto the downward facing side of the panels.

The container itself increased the loads on the panels compared with similar ground-mounted systems, as shown in Figure 5-11. The aerodynamics of the container generated an increased net upward pressure onto the panels.



Figure 5-10 Failures of solar panels mounted on shipping containers

The solid container redirects airflow around it, accelerating the flow onto the solar panels mounted above it. The solar panels' increased height means they are also impacted by higher velocity air than ground-mounted inclined panels, as shown in Figure 5-11.

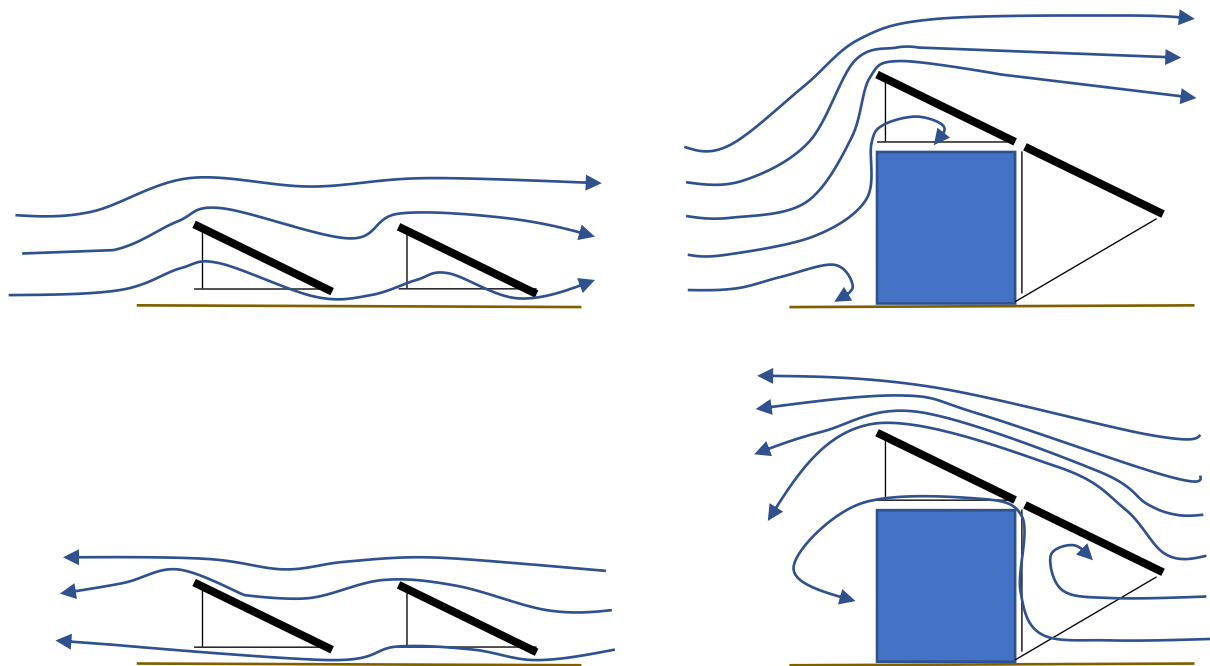


Figure 5-11 Aerodynamic differences between ground-mounted and container-mounted solar arrays

Recommendation

Perform research on the nature of wind loads on solar panel systems mounted on shipping containers. Provide guidance to the solar power industry.

5.4. Roof-mounted solar panels parallel to building roofs

Roof-mounted solar panels are installed on rails fixed to the roof structure through the roof cladding. All the roof-mounted systems observed in the investigation were installed over metal roofs pierced to the roof structure. The solar panel anchorage system involved:

- Clamps that held the solar panel chassis to the rails
- Bolts that anchored rails to the clips
- Brackets under roofing fasteners that anchored the systems to the roof battens

Failures of roof-mounted solar panels were associated with failures of:

- Clamps that held the chassis to the rail
- Roofing fasteners that held the rail to the roofing battens or
- Failure of the batten or its tie-down

5.4.1. Failure of clamps between the chassis and the rails

Failure of the clamps between the chassis and the rails was observed on ground-mounted inclined solar arrays, as discussed in Section 5.2.3. Many similar failures were observed on roof-mounted systems, as illustrated in Figure 5-12. The photos show some loose clamps on the roof sheeting (circled) and some panels remaining on the roof despite the loss of several clamps per panel. Figure 5-7 shows clamps from the same fixing system that were typical of the clamps that were also found on the ground beside this building. The wind direction on this building varied throughout the event, but the last wind direction to have affected the array is shown with the blue arrow.



Figure 5-12 Dislodged clamps from roof-mounted roof systems

The rails on other buildings remained attached to the roof, but the clamps were missing, as shown in Figure 5-13. Loss of clamps was the most common type of failure for roof-mounted solar panels. This roof experienced winds primarily from the direction indicated by the blue arrow. A rail above the one shown was missing as the brackets had pulled the fasteners out of the purlins. In Figure 5-13 the rail obscures the row of fasteners that had been affected by the loss of the top rail.



Figure 5-13 Total loss of clamps and one rail

5.4.2. Failure of the roofing fasteners

Figure 5-14 shows roofs where the rail brackets had removed the roofing screws from the top hat battens, leading to the complete loss of the rails (their original position is indicated by the yellow lines). In some cases, the loss of roofing screws also compromised the performance of the roof sheeting, but in the roofs shown in Figure 5-14, the roofing remained attached to the roof battens. Red circles highlight the missing roofing fasteners. In the upper photo, two rails are missing, but the missing screws that previously held the lower of the two missing rails are obscured by the remaining upper rail. The blue arrow shows the wind direction that caused this damage.

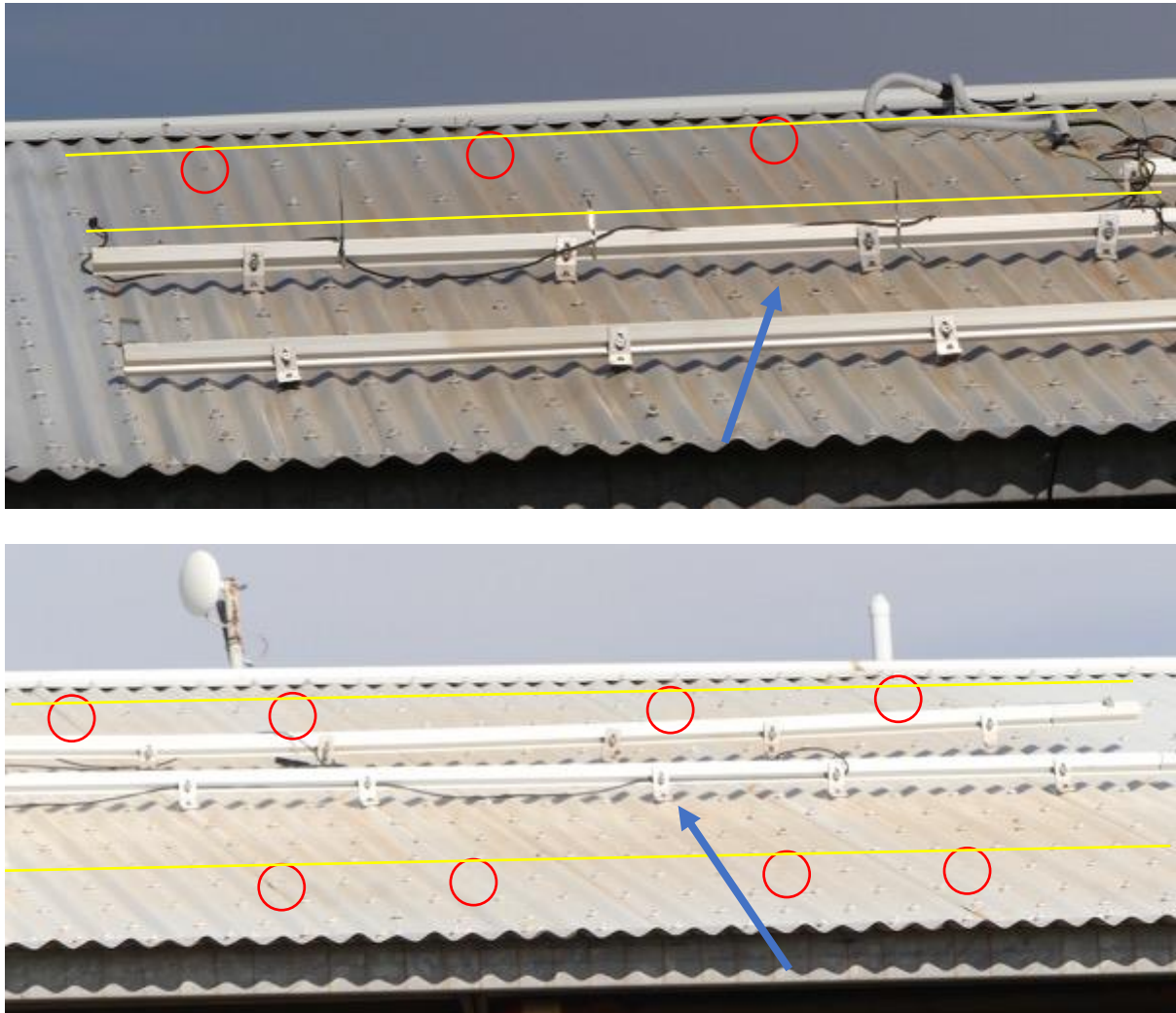


Figure 5-14 Roofs with missing rails and roofing screws

5.4.3. Structural damage to roofs under solar panels

The battens and batten straps under the solar panels on one building failed (Figure 5-15). The solar panels had previously extended across the region that was damaged. The wind direction that appeared to cause the damage is indicated by the blue arrow.



Figure 5-15 Failure of battens and batten straps under solar panels (image courtesy of Warrawagine Station)

This building was around the same age and almost identical construction to two other similar buildings on the same site that did not have solar panels. The roofs without solar panels were not damaged, and none of these buildings had openings on the windward side.

Parackal et al., (2023) present data showing that solar panels can increase the loads on battens in roof structures under roof-mounted panels. The roof discussed above is one in which the increase in loads may have caused the failure of the roof with the solar panels compared with similar roofs without the panels.

Recommendation

Perform research on wind actions on solar panels and the roof structure for a wide range of roof-top configurations. Use the results to review the pressure coefficients on solar panels in AS/NZS 1170.2:2021.

5.5. Debris damage

The faces of solar panels are vulnerable to damage from wind-borne debris. Figure 5-16 shows typical damage from trees or debris from damaged buildings.

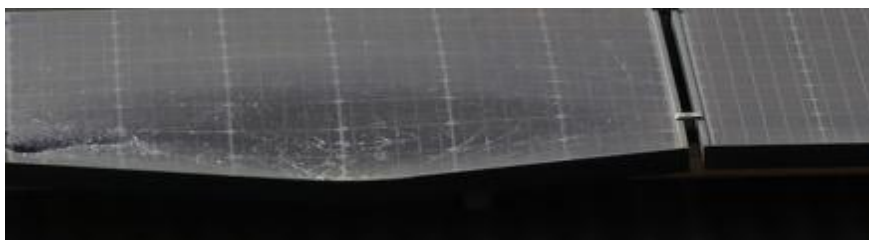


Figure 5-16 Example of damage to solar panels by wind-borne debris

Figure 5-17 shows damage caused by the impact of other solar panels that had become wind-borne debris.

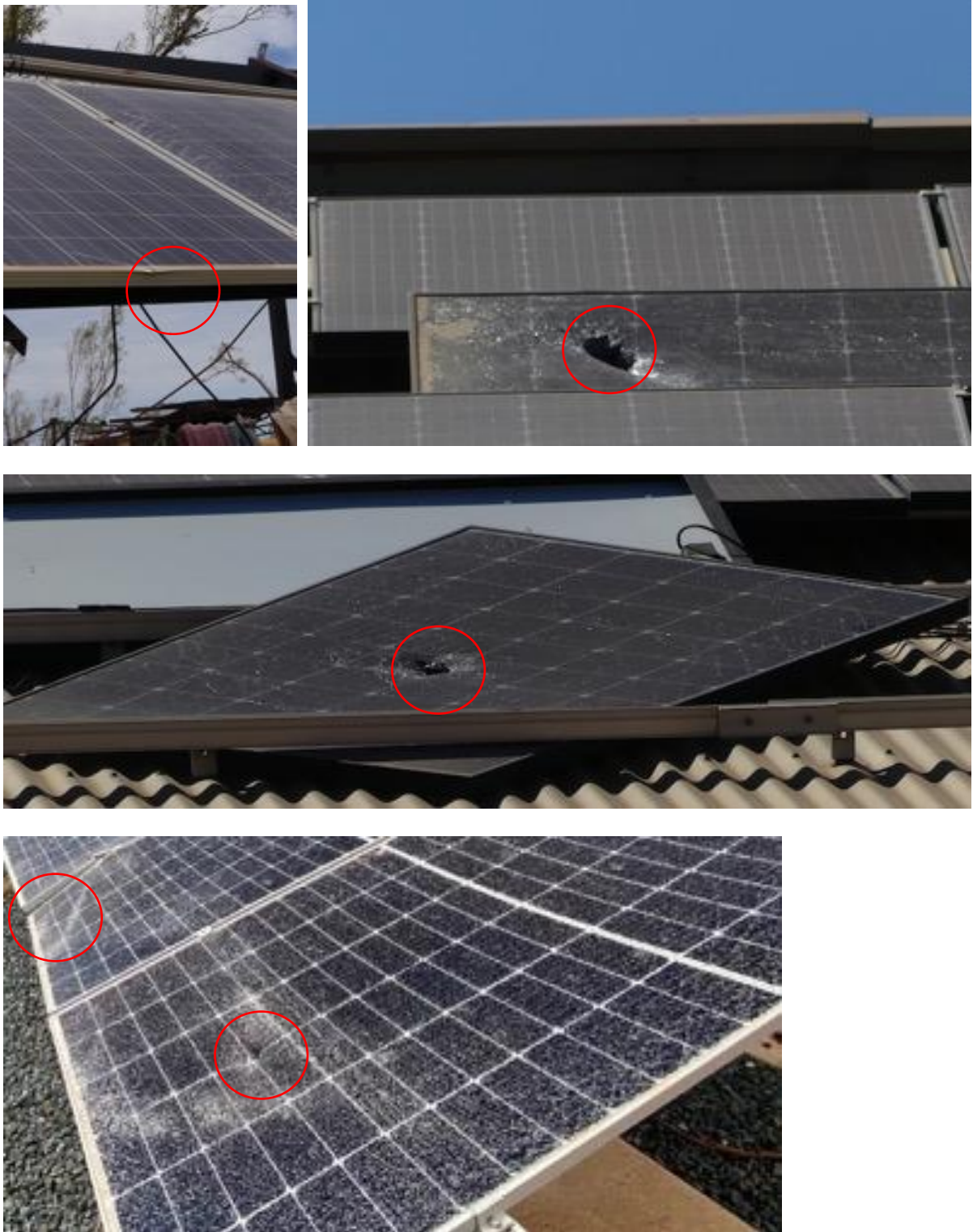


Figure 5-17 Examples of debris damage by other solar panels

5.6. Structural Design criteria for solar panels

Damage to solar panels observed in the study had several safety implications:

- Where the panels detached from their fixings, they became sharp edged, wind-borne debris. Solar panel debris impacted other buildings, fences and facilities. The structural performance requirements in the NCC make it clear that buildings should avoid causing damage to other properties. To be consistent in protecting occupants of other buildings, the same criteria should also apply to attachments to buildings such as solar panels.
- If the system's failure removed fasteners or sheeting from the roof, the structural performance of the building was compromised.
- After the event, damaged solar installations had to be electrically isolated to prevent injury.
- Where the panels were the sole source of power for a facility, such as a communication tower, it compromised the ability of remote communities to communicate in an emergency.

Damage to solar panels observed in the study also had operational implications. It is likely that different installations have different needs. For example, a PV system supplying power to a communications system in a remote area may be of higher importance than a PV system supplementing power to a house that also has grid connection. So, just as the NCC requires designers to consider the importance level of the building they are designing, "importance criteria" needs to be applied to design appropriate levels of resilience for the PV system. These criteria should address issues such as:

- whether the solar array is the only power source
- whether a backup generator is available after an extreme event
- how quickly replacement parts can be sourced to return the system to operation, (which in regional and remote areas can be several months).

Recommendation

Design solar systems (including the panels, their fixings, and their frames) to the same importance level as either the buildings they are mounted on, or in the case of ground-mounted systems, buildings nearby. Design criteria should also consider whether the system needs to be operating after an extreme event.

6. Performance of sheds

Most communities visited in the investigation included sheds that housed activities important to the core business of the community – vehicle repair functions; storage of chemicals, equipment or materials; electricity generators or battery storage; vehicle protection or warehousing functions. In many cases, the value of the equipment stored in the shed exceeded the cost of the shed. In other cases, damage to the shed caused loss of stored equipment or materials and significant interruption to the business.

A high percentage of the sheds in the study area were damaged. Figure 6-1 presents examples of the type of damage caused by wind. The damage ranged from loss of flashings to total loss of the shed and its contents.

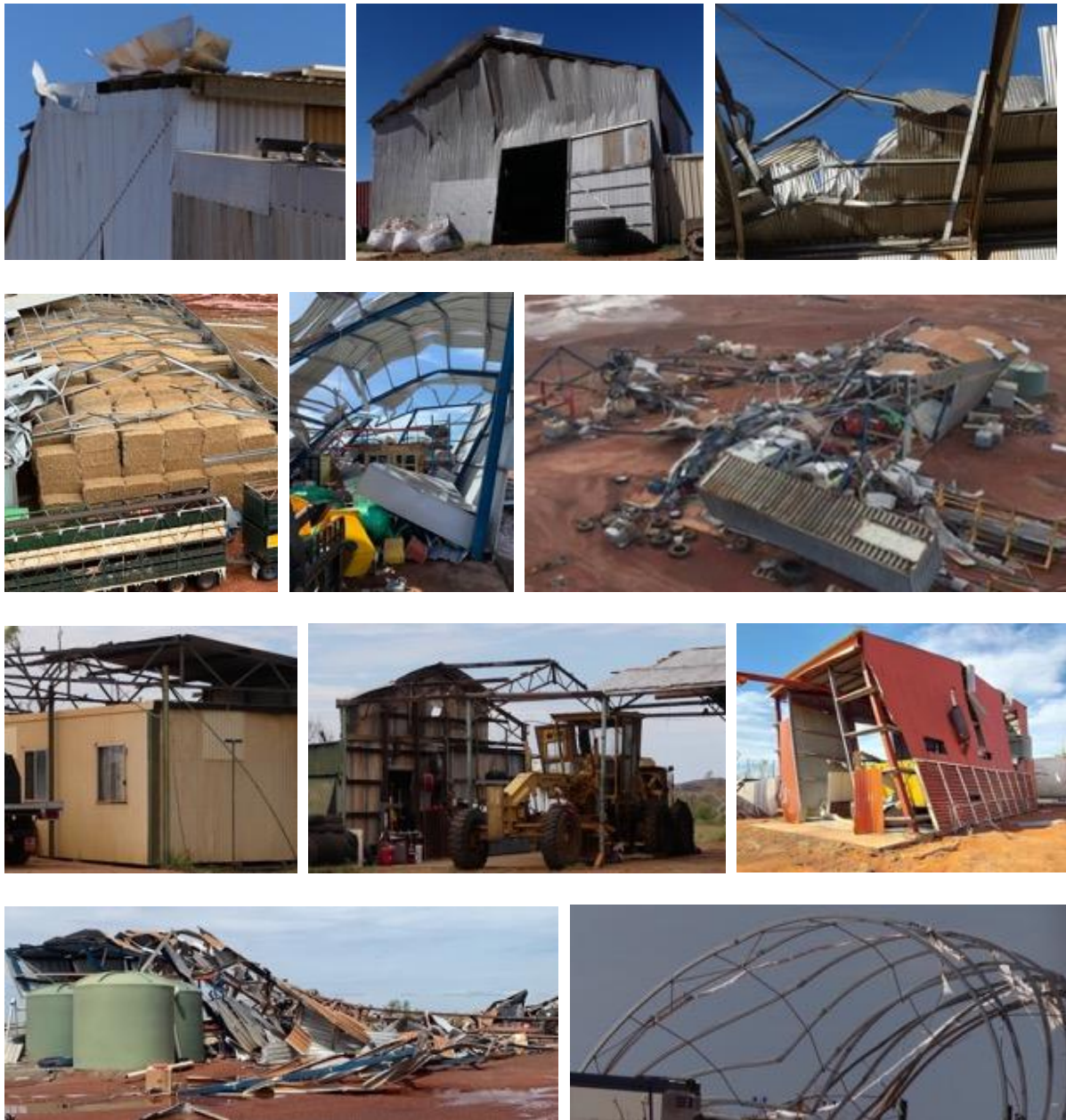


Figure 6-1 Damage to sheds (includes photos supplied by Pardoo station and Warrawagine station).

6.1. Maintenance issues

Signs of corrosion in sheds are often not addressed in routine maintenance and yet they can compromise performance. Figure 6-2 shows where a small shed had been positioned before the cyclone. The hold-down consisted of a steel clamp that held a square hollow section (SHS) frame member to the top of the concrete slab. The clamping brackets (circled) can still be seen in the upper two photos, but the SHS framing almost completely disintegrated due to corrosion.

The disconnection of the hold-down brackets from the shed frame meant that the shed, complete with shelving, was lifted off its original position. The air-borne shed damaged other buildings, as shown in the lower photographs. The damage included roof and wall damage and damage to the contents of both buildings.



Figure 6-2 Corrosion at the base of a small shed and damage to nearby buildings.

Figure 6-3 shows photos of sheds and shelters in a location close to the sea. The prevailing winds mean that salty air passes around these steel-framed buildings for most of the year. The steel rectangular hollow section (RHS) framing members showed significant signs of corrosion, though the relatively thin roofing showed only signs of surface deterioration. However, in many places, there was extensive corrosion of the RHS members around the roofing screws, and in some places, there were holes at least 10 mm in diameter where the screws should have been. This allowed some roofing screws to pull out of the RHS members leading to the loss of parts of the roofing.

In the upper photos in Figure 6-3, corrosion can be seen on the face of the RHS members. Some of the roofing screws pulled out of the corroded RHS (indicated by circles) and this led to the overstressed cladding pulling over adjacent screws, where the corrosion of the RHS was less advanced. The detail of the RHS can be seen in the lower photos.



Figure 6-3 Corrosion in members of shelters close to the sea

Some older sheds used timber components as purlins; in some cases, the timber had deteriorated. This is the case in the shed shown in Figure 6-4.



Figure 6-4 Deterioration of timber in shed elements

Recommendation

Regularly inspect structural elements for signs of deterioration and repair or place as necessary.

The welds in some older sheds were of poor quality. An example is shown in Figure 6-5. In this shed, welds at the top of columns did not have sufficient strength, and it led to the failure of most of the roof structure.



Figure 6-5 Failure of welds at the top of columns

6.2. Lightweight shed systems

Several relatively recently constructed sheds experienced significant wind damage. It is important to consider the effects of internal pressure, even for sheds with permanent openings. Figure 6-6 shows a relatively lightweight shed with completely open ends. At the time of TC Ilsa, the shed was full of hay and had trucks parked across each end. The blockage inside the shed from the contents would have given an internal pressure that the original shed may not have been designed for. The damaged elements included sheeting, purlins, and portal frames.



Figure 6-6 Failure of a recent open-ended shed

Recommendation

Design open sheds with an appropriate net pressure coefficient assuming 'blocked under', as the contents of the shed may increase the pressure on the underside of the roofing.

Figure 6-7 shows sheds of different sizes with very lightweight panels. The shed in the left-hand photo used top-hat framing members spanning 4 m. The shed in the photo on the right shows purlins without any bridging with large spans and insufficient capacity to resist the wind actions. These details were not suitable for wind region D.



Figure 6-7 Lightweight sheds with very light elements

6.3. Curved roofs

Fabric-covered curved structures, such as the shelter shown in the upper photo of Figure 6-8, are used extensively throughout the Pilbara. All three structures shown in Figure 6-8 were exposed to at least one wind direction from the side of the barrel vault roof. The structure in the upper photo had the fabric covering on throughout the cyclone with maximum wind 0.2-sec gust speed of 38 m/s. The fabric had been removed from the lower left roof before the cyclone, but wind gusts from the side estimated at 55 m/s had damaged the unclad frame. The fabric had not been removed from the frame in the lower right-hand photo, and it experienced wind gusts estimated at 65 m/s. The frame was significantly damaged, and the fabric shredded.

Based on wind tunnel tests, the pressure coefficients for the windward side of curved roofs were significantly changed in AS/NZS 1170.2:2021. The failures shown in the lower photos each reflect significant positive pressure on the windward side and negative pressure on the leeward side, aligning with the standard's new pressure coefficients.



Figure 6-8 Fabric-covered, curved roof shades

Recommendation

Remind the building industry that pressure coefficients in AS/NZS 1170.2 for curved roofs have changed.

6.4. Racking failures

Figure 6-1 showed damage to many sheds, where most failures were caused by uplift loads. Figure 6-9 shows two views of a shed with racking failure. In this case, the tall shed had full-height openings on each end to accommodate the crane rail. The large surface area on the wide faces gave significant lateral load, but no bracing was observed on the shorter side walls.



Figure 6-9 Racking failure of a tall shed

There was also a significant lateral component to the failure of the shed on the right-hand photo in Figure 6-7. These cases underline the importance of lateral load-resisting systems in sheds. Even where a shed is designed to be open, it is possible that blockage from stored contents create lateral pressures on the structural system.

Recommendation

Ensure all sheds have adequate wind lateral load capacity (bracing).

7. Performance of Dongas

The term “donga” in Australia means transportable accommodation. Transport limitations often dictate the dimensions of dongas. They were originally designed to be transported on the back of trucks, set up on concrete blocks and connected on site to power, water and sewer quickly to provide temporary construction camps that could be inexpensively relocated. The basic units are around 3.5 m wide to allow easy transportation. The term can now apply to residential buildings such as the dongas illustrated in Figure 7-1 or to larger buildings such as mess halls or gymnasiums where a large open space can be created by joining several dongas together, as shown in Figure 7-5.

Because dongas are lightweight structures, they must be tied down using chains, clamps, or cables to heavy concrete footings or screw piles in various configurations. Where there are deficiencies in the anchorage of the dongas, they can be moved horizontally during cyclones, as shown in the left-hand photo of Figure 7-1, or rolled, as shown in the right-hand photo of Figure 7-1.



Figure 7-1 Dongas that have moved under wind actions

At several Pilbara stations, dongas are used for accommodating workers or visitors; these are often second-hand dongas that have been relocated. Figure 7-2 shows dongas intended for permanent accommodation; the dongas shown on the right are new buildings that were being installed at the time of the cyclone.



Figure 7-2 Dongas for permanent accommodation

There are three main elements in the performance of dongas under wind actions:

- The strength of the prefabricated building itself
- The capacity of the anchorage to the ground to resist horizontal, uplift and sliding forces
- The adequacy of any additional features, such as verandas, that are installed onto the donga once it is in position. These additional features cause extra loads on the donga itself too.

7.1. The capacity of prefabricated dongas

The design and prefabrication of dongas are undertaken to specific design criteria, which are noted on a plate fixed to the outside of the donga. Figure 7-3 shows some rating plates observed in the study with the wind rating highlighted. Note the gravel blasting of both the plate and the paintwork on the donga in the right-most photo.

Unfortunately, the wind ratings have no agreed format, and the three plates show different methods. However, it is possible to obtain an interpretation of the rating provided by contacting the manufacturer. The information on the rating plate is vital to ensuring that a second-hand donga will be appropriate for use in a new location.



Figure 7-3 Wind rating plates on dongas

The wind ratings shown on intact dongas in the study indicated that the donga was appropriate for the site. However, the rating plates for dongas that had been structurally damaged could not be found. Figure 7-4 shows some examples. If there were originally rating plates, they had been lost on some of the panels that had blown away. Some damaged dongas might have been second-hand dongas brought in from an area with a lower wind classification.

Recommendation

Order new dongas that have wind ratings appropriate for the site's wind region, terrain, and topography.

Ensure that the wind rating of any second-hand donga is appropriate for its new location and that it has a thorough structural check to ensure that all structural systems are still fit-for-purpose.



Figure 7-4 Structurally damaged dongas on which no rating plate could be found

In some cases, there were issues associated with the joins between the individual units where larger buildings had been assembled from several individual prefabricated units. Figure 7-5 shows a building constructed from 3 separate units. The blue arrow in the left-hand photo shows the wind direction when the damage was done. The windward unit lost a side wall and its roof. The side wall came to rest around 200 m away, but the roof was not found. The photo on the right was taken looking towards the rest of the building from the resting place of the side wall. While the damaged roof and side wall elements had significantly higher negative pressures because of their proximity to the windward wall, the modular nature of the construction did not allow the adjacent elements to contribute to their strength. The other elements were able to cope with the very high internal pressures that would have come with the loss of part of the windward unit and the collapse of the windward wall.



Figure 7-5 Damage to a single unit within a larger building

Some dongas had window protection. The left-hand photo in Figure 7-2 and Figure 7-6 shows a donga with windows that were protected by debris screens installed with an adequate standoff. These screens and the use of security-rated doors contributed to the resilience of those dongas.



Figure 7-6 Example of an effective debris screen

By contrast, unprotected windows are illustrated in Figure 7-7, together with doors that did not have the capacity to resist the appropriate wind actions – in this case, side wall negative pressures.



Figure 7-7 Damage to windows and doors

Unprotected windows were at risk of damage from wind-borne debris. Although the donga should be designed for the full internal pressure that would result, the broken glass and water ingress through the opening would compromise the building's function. Figure 7-8 shows two different screens installed too close to the window to offer debris protection. In both cases, debris struck the screen and pushed it back far enough to break the glass.



Figure 7-8 Broken windows because the deflection of the screen hit the glass

Recommendation

Use appropriate standoffs for any debris impact screens.

7.2. Capacity of donga anchorage

A structural connection is required to anchor the prefabricated unit to the ground. In many cases, the anchorage is achieved by chains, which allows some flexibility in the site positioning of the prefabricated unit. However, where there was some slack in the chain, the donga could move under wind loads, which often broke pipes or moved the donga off the footings. Figure 7-9 shows dongas that had moved a few hundred mm under lateral wind actions.



Figure 7-9 Building movement accommodated by slack in chains

The upper photo shows a donga that had moved sideways and rotated in plan (particularly obvious from the slope of the veranda posts). The lower photo shows a donga that had moved lengthways by more than 200 mm – enough to break sewer and water pipes.

Anchorage elements are close to the ground and out of sight where signs of corrosion may be difficult to check. The left-hand photo in Figure 7-10 shows an anchorage chain that has started to corrode, but still had sufficient capacity to arrest the movement of the donga. The right two photos show a chain that had corroded through and allowed the donga to roll.



Figure 7-10 Corrosion of anchorage elements

Figure 7-11 shows an option for clamping the donga chassis to the footings. In this case, the footings were not large enough to resist the lateral loads and moved around 50 mm.



Figure 7-11 Clamped donga anchorage

Recommendation

Regularly inspect structural elements for signs of deterioration and repair or replace as necessary. Ensure footings are adequate.

7.3. Verandas and other attachments to dongas

To offer protection from the weather, verandas are often attached to dongas on the side that has the entrance doors. The verandas are not an integral part of the donga and use posts for support on one side and are attached to the donga chassis through the skin on the other side. Verandas were often damaged even though the donga itself sustained minimal damage. In some cases, the damaged veranda caused debris damage to either the donga it was initially attached to or another one.

The damage to the veranda was generally caused by:

- Design of the veranda to a lower wind rating than the donga itself
- Deterioration of the veranda over time
- Overloading the chassis of the donga with the extra load from the added veranda.



Figure 7-12 Veranda damage

The left-hand photo in Figure 7-12 shows a veranda that has started to become detached due to corrosion at the base of the posts (shown in the centre photo). Where steel veranda posts are directly cast into concrete, corrosion seems to be accelerated near the steel/concrete interface. The photo on the right shows veranda posts that have only corroded through near the concrete surface, and this is an area that is easy to inspect.

Recommendation

Verandas attached to dongas should be designed to the same wind rating as the donga and regularly inspected for signs of deterioration.

7.4. Maintenance issues

In addition to the deterioration of the anchorage and veranda elements, some structural elements of the dongas had also deteriorated. The left-hand photo in Figure 7-13 shows the timber bottom plate of an older donga that had rotted. The nail holding capacity of the bottom plate had decreased so the cladding had come off due to negative wind pressure. In the right-hand photo, the flashing was not adequately maintained, and it lifted. This led to damage to the external cladding and water ingress. When repairing this donga, it is vital that all the structural elements in this donga are dried out and checked to prevent the kind of deterioration illustrated in the left-hand photo.



Figure 7-13 Deterioration of structural elements in old dongas

Recommendation

Regularly inspect structural elements for signs of deterioration and repair or place as necessary.

8. Performance of other buildings

This section discusses the performance of enclosed buildings and houses in some remote communities, including cattle stations. There would have been severe damage to many houses and other buildings if TC Ilsa had crossed at Port Hedland or Broome.

8.1. Resilient features

Many buildings in the study region performed well. Several owners or occupants indicated their buildings had been designed to withstand wind region D winds, even though they weren't in region D. Figure 8-1 shows a roof on a building in wind region C that had been designed to a wind region D specification and remained undamaged despite receiving wind speeds over 110% of the wind region C design wind speed. The region D specification used stronger roof battens, tie-down connections with a higher capacity, and closer roofing fastener spacings than those required in wind region C for the same building.



Figure 8-1 Roof with closely-spaced fasteners performed well

Figure 8-2 shows some cyclone shutters permanently installed on homesteads on some cattle stations. During TC Ilsa, these shutters were locked in the downward position and offered protection for the windows and walls behind them.



Figure 8-2 Cyclone shutters protected windows

Building owners who specified resilient features in their buildings (including design for a higher wind region) checked their buildings prior to the cyclone season and regularly performed maintenance to ensure long-term resilience of the buildings.

Figure 8-3 shows a heritage building on a remote station that had been structurally upgraded with a new roof, roof structure and tie-downs. It was undamaged in TC Ilsa, and its performance could be contrasted with a different stone building on the same property that had not yet had a roof and tie-down upgrade (see Figure 8-4).



Figure 8-3 Upgraded tie-down connections on a heritage building



Figure 8-4 Wind damage to a heritage stone building that hadn't yet been upgraded

8.2. Roof sheeting to batten failure

Figure 8-5 shows photos of a building where the roofing fasteners had pulled out of the battens and caused extensive loss of the roof sheeting. The consequences of the roofing loss are shown in Figure 8-6.

Steel battens and roofing fasteners need to be appropriately sized and spaced to resist the design loads. Product manufacturer manuals indicate the correct size, thickness and spacing of elements and provide span tables for different wind loads

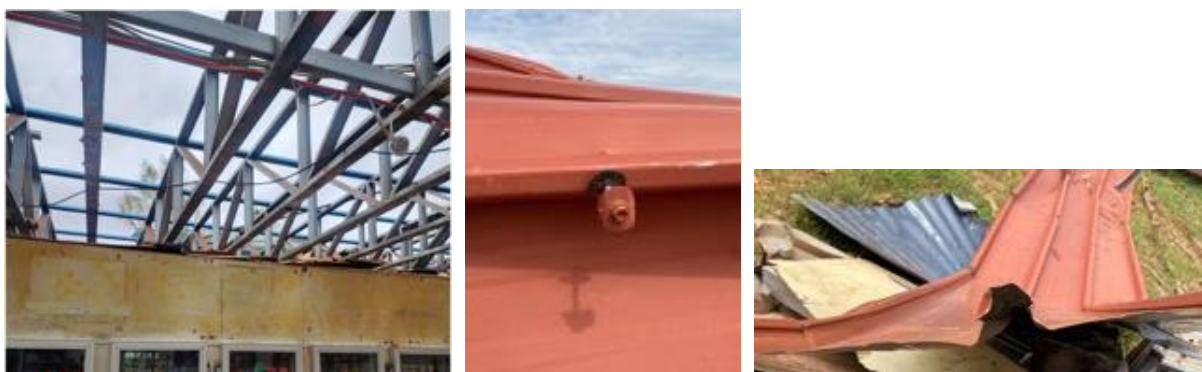


Figure 8-5 Roofing fasteners pulled out of battens



Figure 8-6 Consequences of roofing loss (photos courtesy of media supplied by Pardoo Roadhouse and Tavern)

Recommendation

Ensure that the thickness of light gauge steel elements is appropriate for the loads calculated for each connection.

8.3. Failure of batten to rafter or truss connections

Figure 8-7 shows that nails were used in the batten to truss connections in this house in wind region D and the consequences for the inside. There are few cases in which AS 1684 (Standards Australia, 2010) indicates that nails can be used as batten to rafter connections in any wind region and none for typical batten spacings in wind region D.



Figure 8-7 Nailed batten to truss connections

8.4. Veranda failures

Verandas on the windward side of buildings have high net uplift due to the combination of high positive pressure on the underside of the roof sheeting and high negative pressure on the upper side. Unfortunately, verandas are often not designed correctly for the location, and the consequences of premature failure are not considered. Figure 8-8 shows the failure of the veranda beam to post connections at the steel brackets on a building in wind region C. The veranda post shown in Figure 8-9 travelled more than 40 m with its footing still attached.



Figure 8-8 Failure of veranda beam to post connections



Figure 8-9 Veranda post and footing

8.5. Roof-mounted items

Functional communication technology is essential for remote communities.

In some cases, damage to the satellite dish installation caused damage to roof sheeting if the connection was inadequate. Figure 8-10 shows a satellite dish well-connected to the roof structure and a ground-mounted satellite dish that both performed well during TC Ilsa.



Figure 8-10 Satellite dishes

Figure 8-11 shows some aerials mounted on buildings that performed well, even though parts of the building were damaged. The photo on the left is a two-way radio transmitter fixed to a roof with some damage originating at the roof overhang. The photo on the right shows an aerial of a building with damage to flashings.



Figure 8-11 Examples of aerials that performed well during TC Ilsa

8.6. Implications for buildings in remote communities

In normal travel conditions, it can take a full day of driving to relocate from remote communities and stations to avoid an approaching tropical cyclone. If it has been raining in the lead-up to the cyclone, watercourses may have risen to make the exit roads impassable. These two effects together make it more important that people in remote communities have appropriate buildings in which to shelter in place. These buildings should be sited well above expected flood levels and should be designed to be a place of last resort. This includes:

- Design for a higher importance level – at least importance level 3.
- Design using full internal pressure – regardless of the requirements for the wind region in which it is located.
- Protect windows using screens with appropriate standoffs.
- Use at least security doors to give extra resistance to both wind forces and wind-borne debris.
- Use debris-resistant materials for the walls and ceilings of compartments in which people will shelter.

The designated places of last resort should be sized to offer protection to all the people in the community. At present, there is no incentive for communities to develop these shelters, but funding for them will significantly increase the resilience of the communities.

Recommendation

Provide publicity and incentives for the construction of cyclone-resistant shelters in remote communities. Build new facilities or strengthen specific parts of existing buildings using the design criteria listed above.

9. Conclusions

9.1. Wind field

The Bureau of Meteorology (BoM) accurately predicted the path of TC Ilsa. Two offshore BoM Automatic Weather Stations (AWS) recorded wind speeds for part of the event. Only one AWS was close to the path of the cyclone over land, so ground truthing using vegetation and road signs was required to verify the track and estimate wind speeds in the area affected by the cyclone. The completed wind field used this data and a double Holland model to estimate wind speeds throughout the study area. The same model indicated that because TC Ilsa crossed the coast near low tide, the estimated storm tide was around 1 m above the Highest Astronomical Tide level. Measurements confirmed this and there were no reports or observations of damage due to storm tide.

TC Ilsa crossed the coast with wind speeds close to V_{500} for wind region D. The wind speeds near the track through wind region D remained close to V_{500} . However, as TC Ilsa crossed the WA coast on the northern boundary of wind region D, it caused wind speeds of 124% of V_{500} for wind region C just north of the crossing point. Several facilities in wind region C near the crossing point had been designed to wind region D criteria. The good performance of these buildings underlines the value of building beyond the minimum criteria in the NCC in the areas that are very close to wind region boundaries.

TC Ilsa maximum wind speeds in the part of wind region C that is between 50 km and 100 km from the coast were around 110% of V_{500} for wind region C. The highest wind speeds in wind region B2 were also around 110% of V_{500} . TC Ilsa maintained strength as it passed further inland, so the 0.2-sec standard condition peak gust wind speeds were higher than 120% of V_{500} for an area in wind region A close to the wind region B boundary. The ratio between the estimated wind speed and the design wind speed in parts of wind region A was higher than in the other wind regions.

TC Ilsa caused wind speeds close to or above the V_{500} design wind speeds along much of its track. If it had crossed a major population centre such as Port Hedland or Broome, the extent of damage to communities and buildings would have been even more significant.

9.2. Solar panels

This investigation evaluated the performance of solar panels under wind actions because photovoltaic (PV) solar panels are widely regarded as a key part of Australia's path to energy sustainability. One system located close to landfall, and experienced close to the highest wind speeds estimated in TC Ilsa, sustained no damage, and remained operational after the event. However, eighteen out of nineteen large solar panel systems inspected within the zone that experienced 0.2-sec gusts at 10 m height greater than 40 m/s were damaged during TC Ilsa. Many released significant and dangerous wind-borne debris during the cyclone. Most of the damaged systems were in areas that experienced wind gusts less than V_{500} .

Container-mounted systems experienced higher net pressures than either ground-mounted systems or roof-mounted systems. Guidance and quality assurance in the industry is needed for these systems.

The glazing thickness and edge restraint on some solar panel systems were not adequate to resist the net pressures on the panels on ground-mounted and container-mounted systems. The PV panels must demonstrate the capacity to resist net pressures across the panels appropriate to the site's design wind speed.

The fixings of several systems were not capable of resisting repeated wind gusts. Some chasses tore at holes used to fix the panels to frames or to clamps. In some cases, clamps moved under wind actions and allowed the panels to escape. Fastening systems for solar panels in tropical cyclone areas should demonstrate performance under wind load cycles. A future research project should evaluate a suitable test sequence.

To ensure that no part of the PV system becomes a source of wind-borne debris that could pose a risk to other buildings and their occupants, the design criteria for the solar panel system including its support and tie-downs must be the same as the design criteria of the building it is fixed to, or in the case of ground-mounted systems, nearby buildings.

In addition, the solar panel industry, and system owners need to consider the operational requirements of PV systems in setting the design criteria. It is likely that installations where alternative power sources are not available should have even higher design criteria so they remain operational after an extreme event.

Pressure coefficients in AS/NZS 1170.2 for solar panels should be updated to better protect all configurations of roof-mounted panels and the buildings to which they are anchored.

9.3. Sheds

Several open sheds were severely damaged in TC Ilsa because pressures inside the shed were higher than expected for an open shed as they were filled or partially filled at the time. Open sheds behaved like enclosed buildings with large openings when the contents of the shed effectively blocked the air flow under the roof. Designers of open sheds should anticipate that they may be used for storage and should design them either as an enclosed shed with appropriate internal pressures or as open sheds 'blocked under'.

Design for the appropriate wind region, terrain and topography is also vital for the performance of all sheds.

9.4. Dongas

Some dongas in all wind regions performed well. However, many dongas were damaged because they didn't have appropriate wind ratings for their site, or the tie-downs were not effective. Dongas need to have wind ratings appropriate for the site's wind region, terrain, and topography. Second-hand dongas brought to a site must also have the appropriate wind rating for the characteristics of the new site.

Some larger buildings made of several connected dongas were damaged. There is less opportunity for load sharing in these larger buildings as they do not have as many wall elements per square metre as smaller dongas.

The anchorage of dongas must be taut, well-maintained, and appropriate for the site's design wind speed. Any additions to the dongas, such as verandas, must also be designed and built for the site's design wind speed and be regularly checked and repaired if necessary.

9.5. Other buildings

Many buildings in the study region that performed well did so because they were designed for wind region D, even if they weren't in wind region D. They were also regularly checked and maintained or upgraded if necessary.

The study showed that regular maintenance was required to prevent deterioration of vital structural elements. Steel in contact with the ground or concrete is more prone to accelerated corrosion and requires heavier galvanising and consistent maintenance.

Connection performance in light gauge steel framing members depends on the specification of the appropriate steel thickness. This requirement is important for framing, trusses, battens, and veranda beams.

Some debris screens proved effective in protecting windows, however, appropriate standoffs must be used to ensure that the screen itself doesn't break the window when the screen is hit by wind-borne debris.

People in a number of remote communities had to shelter in place because the travel distance and river crossings meant that they couldn't evacuate when it was known that the cyclone would pose a risk in that location. One or two strengthened buildings in a remote community could provide safe places of last resort. Where these are not already available, some incentives could be provided to fund construction or strengthening of buildings appropriate to become shelters.

10. Recommendations

- Perform research on wind actions on solar panels for a wide range of roof-top configurations, and for panels mounted on shipping containers. Use the results to review the pressure coefficients on solar panels in AS/NZS 1170.2:2021.
- Test solar panel systems using methods that replicate the fluctuating nature of wind loads. Some research may be required to devise an appropriate test method.
- Design solar systems (including the panels, their fixings, and their frames) to the same importance level as either the buildings they are mounted on, or in the case of ground-mounted systems, buildings nearby. Design criteria should also consider whether the system needs to be operating after an extreme event.
- Design open sheds with an appropriate net pressure coefficient assuming 'blocked under', as the contents of the shed may increase the pressure on the underside of the roofing.
- Ensure all sheds have adequate wind lateral load capacity (bracing).
- Remind the building industry that pressure coefficients in AS/NZS 1170.2 for curved roofs have changed.
- Regularly inspect structural elements for signs of deterioration, and repair or replace as necessary.
- Specify new dongas that have wind ratings appropriate for the site's wind region, terrain, and topography.
- Ensure that the wind rating of any second-hand donga is appropriate for its new location and that it has a thorough structural check to ensure that all structural systems are still fit-for-purpose.
- Verandas attached to dongas should be designed to the same wind rating as the donga and regularly inspected for signs of deterioration.
- Use appropriate standoffs for any debris impact screens.
- Ensure that the thickness of light gauge steel elements is appropriate for the loads calculated for each connection.
- Provide publicity and incentives for the construction of cyclone-resistant shelters in remote communities. Build new facilities or strengthen specific parts of existing buildings using the design criteria listed in Section 8.6.

11. References

Australian Building Codes Board (2022) "National Construction Code, Volume 1" Australian Building Codes Board, Canberra.

Bureau of Meteorology (2023) Automatic weather station data available from <http://www.bom.gov.au/wa/observations/waall.shtml> (Downloaded 15 to 16 April, 2023).

Ginger, J., Parackal, K., Ingham, S., Lowe, R., Hildebrandt, C. (2023) "Wind loads on curved free roofs" Proc 21st Australasian Wind Engineering Society Workshop AWES Feb 2 - 3, 2023

Holmes J.D. (2021) "Tropical cyclone impacts on the Western Australian coast" Proc 20th Australasian Wind Engineering Society Workshop AWES April 8-9, 2021

Holmes, J.D. and Ginger, J.D. (2012) "The gust wind speed duration in AS/NZS 1170.2", Australian Journal of Structural Engineering, Vol. 13, No. 3, pp 207-218, <http://dx.doi.org/10.7158/S12-017.2012.13.3>

Parackal, K., Omelaniuk, A., Henderson, D., Ginger, J. (2023) "Wind loads on flush-mounted rooftop solar panels and supporting structural elements", Proc 21st Australasian Wind Engineering Society Workshop AWES Feb 2 - 3, 2023

Risk Frontiers (2023) Summary of TC Ilsa <https://riskfrontiers.com/insights/tropical-cyclone-ilsa-western-australia-dodges-bullet/> (Downloaded 15 May, 2023)

SEA (2020) SEAtide V3.3 User Guide (Qld-Gulf). Jan, 92pp. [Available from: http://www.systemsengineeringaustralia.com.au/download/V3_Qld-Gulf_SEAtide_User_Guide.pdf]

Standards Australia (2010) "AS 1684 series Residential timber-framed construction", Standards Australia, Sydney NSW

Standards Australia (2021) "AS/NZS 1170.2: 2021 Structural design actions – Part 2: Wind actions", Standards Australia, Sydney NSW